# Confronting SUSY models with LHC data via electroweakino production

**Chiara Arina**[1] , **Mikael Chala**[2] , **Víctor Martín-Lozano**[3,4] **and Germano Nardini**[5]

[1] *Centre for Cosmology, Particle Physics and Phenomenology (CP3), Université catholique de Louvain, B-1348 Louvain-la-Neuve, Belgium*

[2] *Deutsches Elektronen Synchrotron, Notkestrasse 85, D-22603, Hamburg, Germany*

[3] *Departamento de Física Teórica & Instituto de Física Teórica UAM/CSIC, Universidad Autónoma de Madrid, E-28049, Madrid, Spain*

[4] *Bethe Center for Theoretical Physics & Physikalisches Institut der Universität Bonn, Nußallee 12, 53115, Bonn, Germany*

[5] *Institute for Theoretical Physics, Albert Einstein Center, University of Bern, Sidlerstrasse 5, CH-3012 Bern, Switzerland*

ABSTRACT: We investigate multi-lepton signals produced by ElectroWeakino (EWino) decays in the MSSM and the TMSSM scenarios with sfermions, gluinos and non Standard Model Higgses at the TeV scale, being the Bino electroweak-scale dark matter. We recast the present LHC constraints on EWinos for these models and we find that wide MSSM and TMSSM parameter regions prove to be allowed. We forecast the number of events expected in the signal regions of the experimental multi-lepton analyses in the next LHC runs. The correlations among these numbers will help to determine whether future deviations in multi-lepton data are ascribable to the EWinos, as well as the supersymmetric model they originate from.

arXiv:1610.03822v1 [hep-ph] 12 Oct 2016

## Contents

## 1 Introduction

The first run of the LHC (Run 1) led to unexpected results. It was a common perception that SUperSYmmetry (SUSY), if related to stabilizing the ElectroWeak (EW) scale, would have been discovered quite quickly while Higgs physics would have needed to wait for higher statistics. However a Higgs boson was found [1, 2] but there is still no sign of physics beyond the Standard Model (SM).

In fact, the collected LHC data impose quite strong bounds on SUSY. First and second generation of squarks and gluinos need to be well above 1 TeV [3, 4]. Sbottoms and stops lighter than about 800 GeV are difficult to accommodate in view of direct search constraints and of the 125 GeV Higgs mass observation, at least in the Minimal Supersymmetric SM (MSSM) [5–8]. Bounds pushing the chargino and neutralino sector well above the EW scale exist as well [3, 4].

Even though these constraints are based on strong model dependent assumptions, there is a general feeling that perhaps the hierarchy problem should be given up. In this spirit, MSSM scenarios where most of the new physics is far away from the reach of the LHC (*e.g.* in high-scale [9], spread [10] or split [11–13] SUSY) are gaining popularity. Nevertheless, before departing towards these drastically fine-tuned scenarios, it is wise to

understand better the model dependence of the experimental bounds. In particular, among several plausible options, it seems sensible to generalize these bounds in frameworks where charginos and neutralinos, somehow protected by the chiral symmetry, feature EW-scale masses, while the beyond-the-SM scalars are in the TeV range and do not interfere with the neutralino and chargino production and subsequent decay.

In SUSY frameworks with only light charginos and neutralinos, dubbed ElectroWeakinos (EWinos) hereafter, the lightest neutralino is the Lightest Supersymmetric Particle (LSP). This particle is an excellent EW scale Dark Matter (DM) candidate. Its relic density reproduces the observed DM abundance in the parameter regions of the Higgs/$Z$-boson funnel and the well-tempered neutralino [14–18]. In the former case the LSP is Bino-like, with mass close to half of the Higgs/$Z$-boson mass. In the latter the LSP is a tuned mixture of gaugino and Higgsinos that achieves the correct relic density away from resonances and coannihilations with non-EWino particles.

At colliders it is the mass gap between the LSP and the other EWinos what differentiates the well-tempered region from the Higgs/$Z$-boson funnel one. Whereas in the former region a compressed spectrum close in mass to the LSP is unavoidable and very hard to probe [19, 20] [1], in the latter a gap of at least $40 \, \text{GeV}$ is guaranteed (by $e.g.$ the LEP chargino mass bound $m_{\widetilde{\chi}^{\pm}} \gtrsim 104 \, \text{GeV}$ [22]). Therefore, provided that EWinos other than the LSP are sufficiently produced, the Higgs/$Z$-boson funnel case exhibits a rich LHC phenomenology with energetic EWino decay products that are easily tagged. In order to characterize this rich phenomenology, in the present paper we determine in detail the multi-lepton plus Missing Transverse Energy (MET) signatures coming from EWinos.

For concreteness we focus on two SUSY models: the MSSM and the TMSSM, $i.e.$ the MSSM supplemented by one hyperchargeless $SU(2)_L$-triplet chiral superfield [23, 24] [2]. In both cases we fix the LSP at the Higgs funnel region while the other EWinos, consisting of Winos, Higgsinos and, for the TMSSM, the fermionic components of the triplet (dubbed Triplinos), are above the chargino mass bound $m_{\widetilde{\chi}^{\pm}} \gtrsim 104 \, \text{GeV}$ [22]. Sfermions and non-SM Higgses are assumed decoupled from the EWino LHC phenomenology but not very heavy in order not to exacerbate the little hierarchy problem. This implies for instance that within the MSSM the 125 GeV Higgs mass is possible only in the large $\tan \beta$ regime, while such a regime is not required in the TMSSM due to the additional $F$ terms increasing the tree level Higgs mass [23, 24]. In these MSSM and TMSSM scenarios we determine the following:

1. *Present bounds on EWinos:* We recast the experimental analyses [31–34] constraining the anomalous production of two or more charged leptons in final states with MET, as it occurs in the production and subsequent decay of EWinos. We then generalize

---

[1]Recently CMS has published a new analysis with the data at 13 TeV to look specifically for soft leptons and set the first constraints on compressed spectra [21].

[2]Among its appealing features (see $e.g.$ Refs. [25–28]), the TMSSM provides a reduction of the little hierarchy problem with respect to the MSSM. In a bottom-up approach, the tuning of the model is similar to the one of the MSSM singlet extension [29] but it can be actually much smaller in appropriate ultraviolet embeddings [30].

the ATLAS and CMS simplified-model constraints to the above MSSM and TMSSM scenarios. This analysis takes an approach similar to the one in Ref. [35].

2. *EWino signatures in future data:* In the parameter space compatible with the present EWino bounds, we produce forecasts for multi-lepton searches. For the whole MSSM and TMSSM EWino parameter regions that we consider, we highlight the number of events that are expected in each Signal Region (SR) of the above multi-lepton analyses. We display results for a luminosity of $100\,\mathrm{fb}^{-1}$ at center-of-mass energy of $13\,\mathrm{TeV}$, nonetheless forecasts for the high luminosity phase are also discussed.

3. *Disentangling the MSSM from other models:* We prove that the correlations among the events commented above are sensitive to the details of the EWino sector. In particular, SUSY models with an extended EWino sector can produce signals whose correlations are not produced by the EWino sectors of other models. Specifically, we prove that there is a small parameter region where the above MSSM and TMSSM scenarios can be disentangled already with $100\,\mathrm{fb}^{-1}$. The region where this disentanglement is possible becomes wide for the luminosity of $3000\,\mathrm{fb}^{-1}$ expected in the high luminosity LHC run.

The rest of the paper is organized as follows. In the next section, Sec. 2, we detail the EW sector of the MSSM and the TMSSM and introduce the parameters and assumptions relevant for our study. Section 3 deals with the technical details of the analyses and experimental searches we use. In Sec. 4 we present the most stringent constraints on the MSSM and the TMSSM EWino parameter space. This sets the basis for our multi-lepton forecasts at the present and future LHC runs, provided in Sec. 5. In this section the possibility of disentangling SUSY models by means of the correlation among multi-lepton signals is also presented. We then come to our conclusions in Sec. 6. We provide further details in Appendix A.

## 2 The SUSY models

In Sec. 2.1 and Sec. 2.2 we briefly describe the EWino sectors of the MSSM and the TMSSM as well as the SM-like Higgs boson emerging in these models. Since we work under the premise that all sfermions, non-SM Higgses and gluinos are at the TeV scale, SM particles and EWinos are the only particles accessible by the LHC. This assumption is supported by the experimental constraints of ATLAS and CMS after Run 1 [3, 4] that tend to push all the scalar SUSY sector to the TeV scale. We also outline the free parameters relevant for our numerical analysis and give technical details about the model implementation in Sec. 2.3.

### 2.1 The MSSM model

The EW sector of the MSSM is constituted by the neutralinos $\widetilde{\chi}_i^0$, with $i = 1, \ldots, 4$, and the charginos $\widetilde{\chi}_j^\pm$, with $j = 1, 2$. In the limit considered in this work, the MSSM is described by four free parameters, $\{M_1, M_2, \mu, \tan\beta\}$, respectively the two gaugino masses, the bilinear

term for the Higgs sector in the superpotential and $\tan\beta = v_2/v_1$ with $v^2 = v_1^2 + v_2^2 = (174\,\text{GeV})^2$, and $v_1$ and $v_2$ being the Higgs Vacuum Expectation Values (VEVs). The mass matrices for the neutralinos and charginos in terms of these four parameters are

$$\mathcal{M}^{tree}_{\widetilde{\chi}^0} = \begin{pmatrix} M_1 & 0 & -\frac{1}{2}g_1v_1 & \frac{1}{2}g_1v_2 \\ 0 & M_2 & \frac{1}{2}g_2v_1 & -\frac{1}{2}g_2v_2 \\ -\frac{1}{2}g_1v_1 & \frac{1}{2}g_2v_1 & 0 & -\mu \\ \frac{1}{2}g_1v_1 & -\frac{1}{2}g_2v_2 & -\mu & 0 \end{pmatrix}, \tag{2.1}$$

and

$$\mathcal{M}^{tree}_{\widetilde{\chi}^\pm} = \begin{pmatrix} M_2 & g_2v\sin\beta \\ g_2v\cos\beta & \mu \end{pmatrix}. \tag{2.2}$$

All the sfermions as well as the pseudo scalar and charged Higgses are much heavier, say in the TeV range. They are then decoupled from the EWino LHC phenomenology. For concreteness we set all the masses of the gluinos, non-SM Higgses, sleptons and 1st/2nd generation of squarks at $2\,\text{TeV}$. All trilinear terms are assumed vanishing. This choice of parameters is in agreement with the current LHC observations.

When the CP-odd Higgs mass $m_A$ is large, the SM-like Higgs mass is given at tree level by

$$m^2_{h,tree} = m_Z^2\cos 2\beta, \tag{2.3}$$

where $m_Z$ is the mass of the $Z$ boson. At loop level, the dominant correction comes from the top squark masses. For stops at the TeV scale, the large $\tan\beta$ regime is the only viable option to achieve $m_h \simeq 125\,\text{GeV}$. We thus fix $\tan\beta = 10$, as we have checked that within the large $\tan\beta$ regime the EWino production and decay are rather insensitive to the specific value of $\tan\beta$.

## 2.2 The TMSSM model

The TMSSM is an extension of the MSSM in which a hyperchargeless $SU(2)_L$-triplet superfield is added. If we express the triplet superfield as

$$\Sigma = \begin{pmatrix} \xi^0/\sqrt{2} & \xi_2^+ \\ \xi_1^- & -\xi^0/\sqrt{2} \end{pmatrix}, \tag{2.4}$$

the superpotential reads

$$W_{\text{TMSSM}} = W_{\text{MSSM}} + \lambda H_1 \cdot \Sigma H_2 + \frac{1}{2}\mu_\Sigma \text{Tr}\,\Sigma^2, \tag{2.5}$$

where the dot $\cdot$ is the $SU(2)_L$ antisymmetric product. The soft breaking Lagrangian can be written as

$$\mathcal{L}_{\text{TMSSM}_{\text{SB}}} = \mathcal{L}_{\text{MSSM}_{\text{SB}}} + m_4^2\text{Tr}(\Sigma^\dagger\Sigma) + \left[B_\Sigma\text{Tr}(\Sigma^2) + \lambda A_\lambda H_1 \cdot \Sigma H_2 + \text{h.c.}\right]. \tag{2.6}$$

We consider no $CP$ violation so the parameters appearing in Eqs. (2.5) and (2.6) are taken as real.

The neutral scalar component $\xi^0$ acquires a VEV $\langle \xi^0 \rangle$. This VEV is very constrained by the EW precision observables that impose $\langle \xi^0 \rangle \lesssim 4$ GeV at 95% C.L. [22, 26]. This limit is naturally satisfied in the parameter region [26]

$$|A_\lambda|, |\mu|, |\mu_\Sigma| \lesssim 10^{-2} \frac{m_\Sigma^2 + \lambda^2 v^2 / 2}{\lambda v} \,, \tag{2.7}$$

where $m_\Sigma^2 \equiv m_4^2 + \mu_\Sigma + B_\Sigma \mu_\Sigma$ is the squared mass term of $\xi^0$. To fulfill this relation, we choose $m_\Sigma = 5\,\mathrm{TeV}$ and $A_\lambda = 0$, while $\mu$ and $\mu_\Sigma$, which we deal as varying parameters, are never taken larger than $1\,\mathrm{TeV}$. Of course, the EWino phenomenology is independent of the specific values of $m_\Sigma$ and $A_\lambda$ we adopt.

**The Higgs sector**  The mixing between the MSSM-like Higgs fields, $H_1$ and $H_2$, and the scalar triplet is negligible for $m_\Sigma \gtrsim 5\,\mathrm{TeV}$ [25]. In this case the EW minimization conditions can be obtained from the scalar potential of $H_1$ and $H_2$. These imply [26]

$$m_3^2 = m_A^2 \sin\beta \cos\beta \,, \tag{2.8}$$

$$m_Z^2 = \frac{m_2^2 - m_1^2}{\cos 2\beta} - m_A^2 + \lambda^2 v^2 / 2 \,, \tag{2.9}$$

$$m_A^2 = m_1^2 + m_2^2 + 2|\mu|^2 + \lambda^2 v^2 / 2 \,, \tag{2.10}$$

$$m_{H^\pm} = m_A^2 + m_W^2 + \lambda^2 v^2 / 2 \,, \tag{2.11}$$

where $m_W$ is the mass of the $W$ vector boson, and $m_1^2$, $m_2^2$ and $m_3^2$ are the MSSM soft parameters of the Higgs fields $H_{1,2}$. In the EW minimum, moreover, the squared mass matrix of the $H_{1,2}$ CP-even Higgs components reads

$$\mathcal{M}_{h,H}^2 = \begin{pmatrix} m_A^2 \cos^2\beta + m_Z^2 \sin^2\beta & (\lambda^2 v^2 - m_A^2 - m_Z^2)\sin\beta\cos\beta \\ (\lambda^2 v^2 - m_A^2 - m_Z^2)\sin\beta\cos\beta & m_A^2 \sin^2\beta + m_Z^2 \cos^2\beta \end{pmatrix} \,. \tag{2.12}$$

Like in the MSSM, for $m_A$ at the TeV scale, all the non-SM Higgses are heavy and the lighter CP-even Higgs, $h$, is aligned to the SM Higgs. Nevertheless, the $h$ tree-level mass

$$m_{h,tree}^2 = m_Z^2 \cos^2 2\beta + \frac{\lambda^2}{2} v^2 \sin^2 2\beta \tag{2.13}$$

can be larger than in the MSSM. Thus, in the TMSSM the little hierarchy problem can be less severe than in the MSSM and can be ameliorated with $\lambda$ of order one and $\tan\beta$ low (in this respect the TMSSM is similar to the singlet extension of the MSSM [29]).

Motivated by the above features, in our analysis we consider TMSSM reference scenarios with $\tan\beta = 3$. We prefer however not to fully exploit the boost in the tree-level Higgs mass [3], consequently we fix $\lambda = 0.65$ and work in a regime where the sfermions, gluino and non-SM Higgses are as heavy as in the MSSM case described in Sec. 2.1.

---

[3] Otherwise stop masses would turn out to be upper bounded by the 125 GeV Higgs mass constraint and possibly too light to be decoupled from the EWino phenomenology.

**The EWino sector** As the TMSSM is an extension of the MSSM with a triplet superfield, not only the scalar sector is enlarged but also the fermionic one. The fermionic components of the triplet augment the number of neutralino states to five and the number of chargino states to three. The Triplinos mix with the MSSM EWinos. The tree-level mass matrices of the neutralino and chargino sector are given by

$$\mathcal{M}^{tree}_{\widetilde{\chi}^0} = \begin{pmatrix} M_1 & 0 & -\frac{1}{2}g_1v_1 & \frac{1}{2}g_1v_2 & 0 \\ 0 & M_2 & \frac{1}{2}g_2v_1 & -\frac{1}{2}g_2v_2 & 0 \\ -\frac{1}{2}g_1v_1 & \frac{1}{2}g_2v_1 & 0 & -\mu & -\frac{1}{2}v_2\lambda \\ \frac{1}{2}g_1v_1 & -\frac{1}{2}g_2v_2 & -\mu & 0 & -\frac{1}{2}v_1\lambda \\ 0 & 0 & -\frac{1}{2}v_2\lambda & -\frac{1}{2}v_1\lambda & \mu_\Sigma \end{pmatrix}, \qquad (2.14)$$

and

$$\mathcal{M}^{tree}_{\widetilde{\chi}^\pm} = \begin{pmatrix} M_2 & g_2v\sin\beta & 0 \\ g_2v\cos\beta & \mu & -\lambda v\sin\beta \\ 0 & \lambda v\cos\beta & \mu_\Sigma \end{pmatrix}. \qquad (2.15)$$

The presence of the Triplino increases the number of the EWino parameters to six, which are now $\{M_1, M_2, \mu, \mu_\Sigma, \tan\beta, \lambda\}$. Among them, only the first four parameters are free once we fix $\tan\beta$ and $\lambda$ as previously described.

The enlarged EW sector can induce deviations in the $h \to \gamma\gamma$ and $h \to \gamma Z$ decay channels while keeping all the lightest-Higgs tree-level couplings SM-like [25]. These deviations are sizeable only if $m_\Sigma \sim 100\,\text{GeV}$ (when $\tan\beta$ is small and $\lambda$ is large), while for $m_\Sigma \gtrsim 300\,\text{GeV}$ they are generally negligible [28]. We use this lower bound on $m_\Sigma$ in our analysis.

The rest of the paper investigates the imprints of the additional EWinos on the multi-lepton searches. The reader interested in other phenomelogical aspects of the TMSSM is referred to Refs. [25–28, 30].

## 2.3 Numerical implementation of the (T)MSSM models

The multi-lepton signatures arise from EWino production and their subsequent decay into the LSP. The charginos and the neutralinos typically decay into $\widetilde{\chi}^0_1$ and a $W, Z$ or $h$ boson, which subsequently can decay leptonically. It should be noted that the current LHC limits strongly depend on the presence of particular decay modes, and are considerably weakened in case of compressed [36] or stealth [37] spectra. For instance the strongest bounds on EWino parameters are obtained with a very light (LSP) Bino mass, $M_1 \sim 10$ GeV, on-shell $W, Z$ and $h$ bosons, and high $p_T$ final state leptons. On the other hand, for $M_1$ above 100 GeV, the Run 1 LHC constraints are actually not much stronger that the LEP bound $m_{\chi^\pm} \gtrsim 104\,\text{GeV}$ [22] (see *e.g.* Ref. [35]).

In our analysis we consider a fixed LSP one-loop mass, namely $m_{\widetilde{\chi}^0_1} = 63$ GeV. This choice of mass implies $M_1$ varying in between approximately 50 and 80 GeV, depending on the particular values of the other EWino parameters. As previously explained, the choice of a 63 GeV pure Bino neutralino is dictated by DM requirements. Indeed in both the MSSM and the TMSSM the Higgs pole is a region where the LSP achieves the correct relic

density and is compatible with DM direct detection searches [28, 38]. At the same time the invisible decay channel $h \to \widetilde{\chi}_1^0 \widetilde{\chi}_1^0$ is closed. This, together with a sensible parameter choice suppressing deviations in the Higgs loop-induced decays (*e.g.* $m_\Sigma \gtrsim 300\,\text{GeV}$), guarantees full agreement with the experimental Higgs measurements [39]. Notice that a slightly different LSP mass would not alter significantly our multi-lepton results, while for a significantly lower value of $M_1$ the constraints will be tighter [35]. Nevertheless in this latter case, for such lower masses, the EWino signals should be also cross correlated to the Higgs invisible width and the spin-independent DM-nucleon exclusion limits.

Both MSSM and TMSSM models we consider are implemented numerically in the following way:

- The models are generated by means of SARAH v4 [40–42], which produces the model files for SPHENO v3 [43, 44] and the UFO files for MADGRAPH5_AMC@NLO [45];

- The particle mass spectrum is computed in SPHENO: all EWino masses are computed at one loop level while the Higgs mass is computed at two loop level. Practically, at each parameter point we consider, we adjust the stop soft masses, which are in the TeV range, to obtain the observed Higgs mass. Concerning the TMSSM we refer to Ref. [28] for the detailed description on how we compute the Higgs mass including the most relevant two-loop contributions;

- The Branching Ratios (BRs) as well as the total decay widths of all particles are computed by means of SPHENO;

- Regarding the TMSSM, we keep $\lambda$ fixed at 0.65 and consider two values for the Triplino mass: $\mu_\Sigma = 300\,\text{GeV}$ in one reference scenario (called TMSSM_1 hereafter) and $\mu_\Sigma = 350\,\text{GeV}$ in another scenario (called TMSSM_2 hereafter). We will comment on the impact of changing $\lambda$ in Sec. 4.

## 3 Searches for EWinos at the LHC: multi-lepton signals

There are several SUSY searches implemented by the experimental collaborations. Relevant to our analysis are mainly those searches involving the direct production of charginos and neutralinos, as these are the only particles in the reach of LHC in our setup. More specifically we consider the searches that have only leptons in the final state, cleaner signatures with respect to jets + MET. We concentrate on 8 TeV data. As a matter of fact, most of dedicated analyses at 13 TeV are either preliminary [46–48] or do not provide stronger constraints in general due to the still small luminosity [49]. At any rate, our results are not expected to be sensibly modified in the short term.

The multi-lepton searches look for departures in particular leptonic final states + MET with respect to the SM predictions. If a deviation is seen, that could be interpreted as the production and subsequent decay to the LSP of EW particles, depending on the specific final state under investigation. The observed number of events in a specific search is typically studied in terms of Simplified Model Spectra (SMS). The SMS rely on the assumptions that only $\widetilde{\chi}_2^0$ and $\widetilde{\chi}_1^\pm$ are produced, that they both have the same mass and

they decay 100% into the LSP plus leptons via specific decay channels (some of them can include a decay mediated by a slepton). Within the SMS interpretation, for instance, the three-lepton searches constrain the chargino mass up to 700 GeV for massless LSP [50, 51].

However if the EW particle content is richer than in SMS approach or the topologies leading to multi-leptons + MET are different, the exclusion bounds from Run 1 on $\widetilde{\chi}_1^\pm$ and $\widetilde{\chi}_1^0$ cannot be naively applied to the model to constrain chargino/neutralino masses. The correct approach in this case is to produce full event simulations at the detector level for all processes leading to a certain final state. In the (T)MSSM, for example, decays into the LSP can produce the following signals:

- $pp \to \widetilde{\chi}_i^\pm \widetilde{\chi}_j^\pm$ (with $i, j = 1, 2, (3)$) and $\widetilde{\chi}_i^\pm \to W^\pm \widetilde{\chi}_1^0$ give rise to two Opposite Sign (OS) leptons when both $W$s decay leptonically;

- $pp \to \widetilde{\chi}_i^0 \widetilde{\chi}_j^\pm$ (with $i = 2, 3, 4, (5)$ and $j = 1, 2, (3)$) and $\widetilde{\chi}_j^\pm \to W^\pm \widetilde{\chi}_1^0$, $\widetilde{\chi}_i^0 \to Z \widetilde{\chi}_1^0$ lead to three-lepton final states when both $W$ and $Z$ bosons decay leptonically, with two leptons being of the Same Flavour and OS (SFOS);

- $pp \to \widetilde{\chi}_i^0 \widetilde{\chi}_j^0$ (with $i, j = 2, 3, 4, (5)$) with $\widetilde{\chi}_i^0 \to Z \widetilde{\chi}_1^0$ gives rise to four-lepton final states, with two pairs of SFOS;

- Also decay chains can contribute to the multi-lepton final states. For instance $pp \to \widetilde{\chi}_3^0 \widetilde{\chi}_3^0$ with $\widetilde{\chi}_3^0 \to Z \widetilde{\chi}_1^0$ and $\widetilde{\chi}_3^0 \to W^- \widetilde{\chi}_1^+ \to W^- W^+ \widetilde{\chi}_1^0$ produce different number of leptons plus MET signatures depending on whether the $W$ and $Z$ bosons decay leptonically.

All these possibilities will be taken into account in our analysis as described below. The relative weight of these decay chains with respect to the two or three body decays into the LSP will depend on the composition of the neutralinos and charginos that are produced as well as on the mass spectrum.

## 3.1 Recasting of the experimental searches

In the following we describe the experimental searches we consider and how they are implemented in our analysis. Among the leptonic searches available we take into account the di-lepton search plus MET, the three-lepton search plus MET and the four-lepton search with MET. The latter is based on the data that ATLAS collected with a luminosity of 20.7 fb$^{-1}$, while the former rely on the selected events collected by the ATLAS detector with a luminosity of 20.3 fb$^{-1}$, all during Run 1 with $\sqrt{s} = 8$ TeV center-of-mass energy. We do not consider the one-lepton and two $b$-jets + MET [52] search, as its sensitivity is not yet competitive with the other leptonic searches. It should be noted however that this search might probe a parameter space which is poorly covered by other SUSY analyses, namely at large $M_2$ and $\mu$ [35].

**Two-lepton + MET search [31]**   This search looks for a pair of OS leptons and MET and has a veto on $\tau^\pm$ leptons in the selected events. In the SMS approach, this search is sensitive to chargino pair production, followed by the decay of the charginos either directly

into the LSP via $W$ boson emission either mediated by sleptons, or direct slepton pair production, depending on the assumption on the SUSY mass spectrum. It is also designed to be sensitive to chargino and next-to-lightest neutralino production, decaying into the LSP via a $W$ and a $Z$ boson, with the $W$ decaying hadronically and $Z$ boson leptonically.

Irrespectively of the flavour, all OS lepton pairs must satisfy the following criteria:

- $p_T > 35$ GeV for the higher-$p_T$ lepton;

- $p_T > 20$ GeV for the other lepton;

- an invariant mass of the di-lepton pair $m_{ll} > 20$ GeV.

Besides $m_{ll}$, another variable to tag the selected events that suppresses the main backgrounds, namely $WW$, $ZV$ (with $V$ a vector boson) and top ($t$) production, is the stransverse mass $m_{T2}$, defined as

$$m_{T2} = \min_{\mathbf{q_T}} \left\{ \max(\mathrm{m_T}(\mathbf{p_T^{l1}}, \mathbf{q_T}), \mathrm{m_T}(\mathbf{p_T^{l2}}, \mathbf{p_T^{miss}} - \mathbf{q_T})) \right\} \qquad (3.1)$$

with $\mathbf{p}_T^{l1}$ and $\mathbf{p}_T^{l2}$ being the transverse momentum of each of the two leptons, $\mathbf{p}_T^{miss}$ the MET vector and $\mathbf{q}_T$ the transverse vector that minimises the larger of the two transverse masses defined as

$$m_T = \sqrt{2(p_T^l p_T^{miss} - \mathbf{p}_T^l \cdot \mathbf{q}_T)}. \qquad (3.2)$$

The end point of $m_{T2}$ is correlated with the difference in mass between the produced particles and the LSP.

In some SRs, the signal events are also selected based on the variable $E_T^{miss,rel}$, defined as

$$E_T^{miss,rel} = \begin{cases} p_T^{miss} & \text{if } \sin \Delta\Phi_{l,j} \geq \pi/2, \\ p_T^{miss} \times \sin \Delta\Phi_{l,j} & \text{if } \sin \Delta\Phi_{l,j} < \pi/2, \end{cases} \qquad (3.3)$$

where $\sin \Delta\Phi_{l,j}$ stands for the azimuthal angle between the direction of $\mathbf{p}_T^{miss}$ and, depending on the case, that of the nearest electron, muon, central $b$-jet or central light flavour jet.

The flavour of the lepton pair depends on the SR, in some case both Same Flavour (SF, $e^+e^-$ and $\mu^+\mu^-$) and Different Flavour (DF, $e^\pm\mu^\mp$) are selected, while in other SRs only SF di-leptons are considered. There are in total seven SRs, each one with specific cuts as follows:

- **SRm$_{T2,90}$**: both SF and DF leptons, $Z$ veto, namely $m_{ll}$ must be at least 10 GeV from the $Z$ boson mass, $m_{T2} > 90$ GeV and $E_T^{miss,rel} > 40$ GeV, zero central and forward light and $b$-jets. The main background is given by $WW$, $ZV$ and $t$ production and is estimated to be 61.5 events;

- **SRm$_{T2,110}$**: same as above with however $m_{T2} > 110$ GeV and an expected of background events of 12.5;

- **SRm$_{T2,150}$**: same as SR-m$_{T2,90}$ with $m_{T2} > 150$ GeV and an expected of background events of 4.2;

- **SRWWa**: both SF and DF leptons, $Z$ veto, $\mathbf{p}_T^{ll} > 80$ GeV, $m_{ll} < 120$ GeV and $E_T^{\mathrm{miss,rel}} > 80$ GeV, zero central and forward light and $b$-jets. This region is designed to look for production of on-shell $W$ bosons, however close to threshold. The main background is given by $WW$, $ZV$ and $t$ production, giving rise to 160.1 expected events;

- **SRWWb**: both SF and DF leptons, $Z$ veto, $\mathbf{p}_T^{ll} > 80$ GeV, $m_{ll} < 170$ GeV and $m_{T2} > 90$ GeV, zero central and forward light and $b$-jets and expected background events of 48.3. This region, together with SRWWc, is designed for charginos with masses larger than 120 GeV and boosted $W$ bosons;

- **SRWWc**: same as SRWWb however with no cut on $m_{ll}$ and $m_{T2} > 100$ GeV and expected background events of 29.3;

- **SRZjets**: SF leptons only, two central light jets (from the $W$ decaying hadronically), the di-lepton invariant mass should be within 10 GeV of the $Z$ boson mass, $E_T^{\mathrm{miss,rel}} > 80$ GeV, $\mathbf{p}_T^{ll} > 80$ GeV, the separation between the two leptons should be $0.3 < \Delta R_{ll} < 1.5$, the two highest-$p_T$ jets are required to satisfy $p_T > 45$ GeV and the invariant mass of the jet pair should be $50\,\mathrm{GeV} < m_{jj} < 100$ GeV. Here the expected number of background events is 1.4.

In our models this search will constrain mostly chargino production decaying via $W$ bosons into the lightest neutralino plus MET, hence the most relevant SRs are SRWWa, SRWWb and SRWWc.

**Three-lepton + MET search [32]** This search looks for the production of chargino and neutralinos, which decay further into three-leptons plus MET in the form of two LSPs and neutrinos. In the SMS approach this search constrains $\widetilde{\chi}_1^{\pm}$ and $\widetilde{\chi}_2^0$, which decay into $\widetilde{\chi}_1^0$ via off or on-shell $W$ and $Z/h$ bosons respectively.

The selected events must contain exactly three leptons, two of them are required to be of OS, while the flavour can be different depending on the definition of the SR (signal electrons or muons are labelled with $l$ and $l'$, where the flavours of $l$ and $l'$ are different). The leptons should be separated from each other by $\Delta R > 0.3$. The selected events should not contain any $b$-jet, however there is no requirement on the number of non $b$-jets. The trigger for the signal leptons depends on their flavour:

- single isolated $e$ or $\mu$: $p_T > 25$ GeV;

- $e^+e^-$: $p_T > 14$ GeV and $p_T > 14$ GeV or $p_T > 25$ GeV and $p_T > 10$ GeV;

- $\mu^+\mu^-$: $p_T > 14$ GeV and $p_T > 14$ GeV or $p_T > 18$ GeV and $p_T > 10$ GeV;

- $e^{\pm}\mu^{\mp}$: $p_T^e > 14$ and $p_T^{\mu} > 10$ GeV or $p_T^{\mu} > 18$ GeV and $p_T^e > 10$ GeV.

To further suppress the background (mainly given by $WZ$, $ZZ$, $VVV$, $t\bar{t}V$ and $tZ$), relevant kinematic variables are $p_T^{\mathrm{miss}}$, $m_{T2}$ and $m_T$ defined in Eqs. (3.1) and (3.2).

**Table 1**. Definition of the bins for SR0τa belonging to the three-lepton plus MET experimental search.

| Bin | $m_{\mathrm{SFOS}}$ [GeV] | $m_T$ [GeV] | $E_T^{\mathrm{miss}}$ [GeV] | Z veto | SM background [# events] |
|---|---|---|---|---|---|
| 1 | 12-40 | 0-80 | 50-90 | no | 23 |
| 2 | 12-40 | 0-80 | > 90 | no | 4.2 |
| 3 | 12-40 | > 80 | $50 - 75$ | no | 10.6 |
| 4 | 12-40 | > 80 | > 75 | no | 8.5 |
| 5 | 40-60 | 0-80 | 50-75 | yes | 12.9 |
| 6 | 40-60 | 0-80 | > 75 | no | 6.6 |
| 7 | 40-60 | > 80 | 50-135 | no | 14.1 |
| 8 | 40-60 | > 80 | > 135 | no | 1.1 |
| 9 | 60-81.2 | 0-80 | 50-75 | yes | 22.4 |
| 10 | 60-81.2 | > 80 | 50-75 | no | 16.4 |
| 11 | 60-81.2 | 0-110 | > 75 | no | 27 |
| 12 | 60-81.2 | > 110 | > 75 | no | 5.5 |
| 13 | 81.2 - 101.2 | 0-110 | 50-90 | yes | 715 |
| 14 | 81.2 - 101.2 | 0-110 | > 90 | no | 219 |
| 15 | 81.2 - 101.2 | > 110 | 50-135 | no | 65 |
| 16 | 81.2 - 101.2 | > 110 | > 135 | no | 4.6 |
| 17 | > 101.2 | 0-180 | 50-210 | no | 69 |
| 18 | > 101.2 | > 180 | 50-210 | no | 3.4 |
| 19 | > 101.2 | 0-120 | > 210 | no | 1.2 |
| 20 | > 101.2 | > 120 | > 210 | no | 0.29 |

In total there are five SRs, defined by the flavour and the charge of the leptons and sometimes requiring the Z veto (no SFOS lepton invariant mass within 10 GeV of the Z boson mass). In each SR the cuts on the kinematic variables are:

- **SR0τa**: $l^{\pm}l^{\mp}l'$, $l^{\pm}l^{\mp}l$, τ flavour veto. This is a complicated SR, with all kinematic variables separated in 20 bins, as detailed in Tab. 1.

We do not consider other SRs reported by the experimental collaboration, as they tag more τ leptons and hence reduce the sensitivity with respect to SR0τa. In our model this search will constrain the production of a chargino and a neutralino (not only $\widetilde{\chi}_1^{\pm}$ and $\widetilde{\chi}_2^0$) decaying directly or via a decay chain into the LSP plus three leptons, depending on the mass spectrum. Only $Z, W$ and the $h$ bosons are considered in the decays, as all non-SM scalars are much heavier.

**Four-lepton + MET search [33, 34]**  This search looks for four or more isolated leptons in the final state plus MET. In the SMS approach this search can constrain the production of a pair of heavy neutralinos, decaying for instance into two $Z$ bosons and two LSPs. In the selected events at least three 'light leptons' are required, where the term 'light lepton' refers to electrons and muons only, including those from leptonic decay of the tau. The

term 'lepton' refers to electrons, muons and taus. Tau leptons that decay hadronically are reconstructed by requiring the jets to have $p_T > 10$ GeV and pseudorapidity $|\eta| < 2.5$.

The invariant mass of all possible SFOS light lepton pairs must be larger than 12 GeV to suppress the background from low energy resonances. The signal is discriminated over the background using the effective mass variable

$$m_{\text{eff}} = p_T^{\text{miss}} + \sum_\mu p_T^\mu + \sum_e p_T^e + \sum_\tau p_T^\tau + \sum_j p_T^j, \qquad (3.4)$$

where $p_T^j$, the transverse momentum of the jets, must be at least 40 GeV. The SM processes that originate the main background are $ZZ$, $ZWW$, $t\bar{t}Z$ and Higgs production. There are in total five SRs, three requiring an extended $Z$ veto and two requiring $Z$ candidates (the updated version [34] contains additional SRs). The extended $Z$ veto is defined as each possible pair, triplet and quadruplet of light leptons in the selected events with an invariant mass between 81.2 GeV and 101.2 GeV to be discarded. The cuts in each region are:

- **SR0Z**: at least four light leptons and no $\tau$ lepton, $p_T^{\text{miss}} > 75$ GeV, SFOS light leptons with an invariant mass between 81.2 GeV and 101.2 GeV. The number of SM background expected events is 1.7;

- **SR1Z**: one $\tau$ lepton and three light leptons, $p_T^{\text{miss}} > 100$ GeV, SFOS light leptons with an invariant mass between 81.2 GeV and 101.2 GeV. The number of SM background expected events is 1.6;

- **SR0noZa**: at least four light leptons and no $\tau$ lepton, $p_T^{\text{miss}} > 50$ GeV, extended veto. The number of SM background expected events is 2;

- **SR0noZb**: at least four light leptons and no $\tau$ lepton, $p_T^{\text{miss}} > 75$ GeV, $m_{\text{eff}} > 600$ GeV, extended veto. The number of SM background expected events is 4.8;

- **SR1noZ**: one $\tau$ lepton and three light leptons, $p_T^{\text{miss}} > 100$ GeV, $m_{\text{eff}} > 400$ GeV, extended veto. The number of SM background expected events is 1.3.

In our analysis this search will constrain heavy neutralino and heavy chargino production decaying two body as well as via long decay chains into the LSP.

## 3.2 Numerical implementation of the analyses

The details on the experimental analysis implementation and the generation of the event simulations for the MSSM and the TMSSM models are the following:

- The event simulations at parton level are produced by MADGRAPH5_AMC@NLO. To be specific, we simulate the production cross section of all possible EWinos with 500k events, *i.e.*: $pp \to Z \to \widetilde{\chi}_i^0 \widetilde{\chi}_j^0$, $pp \to Z/\gamma \to \widetilde{\chi}_k^\pm \widetilde{\chi}_l^\pm$ and $pp \to W^\pm \to \widetilde{\chi}_i^0 \widetilde{\chi}_k^\pm$ with $i, j = 1, ..., 4, (5)$ and $k, l = 1, 2, (3)$;

- The decays of charginos and neutralinos producing the leptonic final states are computed with PYTHIA v6 [53], as well as the showering and hadronization;

- We use DELPHES v3 [54] to simulate the detector response, with the default detector card and modified lepton efficiencies, in order to have a better matching with the experimental searches;

- The experimental analyses are implemented in MADANALYSIS v5 [55, 56]. Each analysis has been validated by considering few clearly defined benchmark points. More specifically the two-lepton + MET search is validated by reproducing figure 5 as well as the benchmark points in tables 5 and 6 of Ref. [31]. The three-lepton + MET and four-lepton + MET searches are validated using the outflow of benchmark points provided by CHECKMATE v1 [57] [4] and SEER [65]. In all cases we find agreement within 20%;

- The exclusion bounds are computed at the 95% confidence level (CL) with the CL$_\text{s}$ method [61]. In the case of the two-lepton search, our analysis takes into account only one SR, SRWWa. The SRs are indeed not independent, they highly and non trivially overlap, hence they cannot be easily combined together with SRWWa in a statistically meaningful way. The constraint coming from the three-lepton analysis considers all the 20 bins of SR0$\tau$a, since they are all statistically independent. In the four-lepton analysis, the first two SRs are not independent, hence we do not consider SR1Z for the constraints. We have checked that SR1Z has no impact on the shape of the exclusion region, as SR0Z contains many more events due to its looser cuts.

## 4   MSSM and TMSSM: excluded regions after the LHC Run 1

Figure 1 illustrates the status of the MSSM and the TMSSM models we consider in the light of the multi-lepton searches of LHC Run 1. In all panels we show the exclusion contours derived from the two, three and four lepton + MET searches in green, pink and blue respectively, in the $\{\mu, M_2\}$-plane. The shaded orange region denotes the exclusion limit at 95% CL on the chargino mass, $m_{\widetilde{\chi}^\pm} > 103.5$ GeV [22]. This bound comes from the search for direct production of charginos at LEP via a $Z$ boson and holds for a generic MSSM scenario. The exclusion limit breaks down if the lightest chargino and neutralino are compressed in mass, in models where the LSP is not the neutralino and in models with R parity violation [66]. In the TMSSM models we consider the bound still holds, as the LSP neutralino is never close in mass with the lightest chargino and $\mu_\Sigma$ is sizeable [66].

The left panel of Fig. 1 illustrates the disfavoured regions for the MSSM scenario with a fixed LSP mass of 63 GeV. The most constraining search is the three-lepton + MET search (pink region), which excludes $\mu$ up to TeV for $M_2 \lesssim 180$ GeV and $M_2 < 380$ GeV for $\mu \lesssim 250$ GeV. The latter region has both $M_2$ and $\mu$ light, which lead to a light and quite compressed mass spectrum for the lightest chargino and for the neutralinos $\widetilde{\chi}_2^0$ and $\widetilde{\chi}_3^0$. Consequently these particles are produced with sizeable cross sections and further decay directly into the LSP via on/off shell two/three body decay. As exemplified by the benchmark point MSSM_p2 in Tab. 2, various processes ($pp \to \widetilde{\chi}_1^\pm \widetilde{\chi}_2^0$, $pp \to \widetilde{\chi}_1^\pm \widetilde{\chi}_3^0$)

---

[4]CHECKMATE uses FASTJET [58, 59], the anti-$k_t$ jet algorithm [60], the CL$_\text{s}$ prescription [61] and the $m_{T2}$ algorithm [62–64].
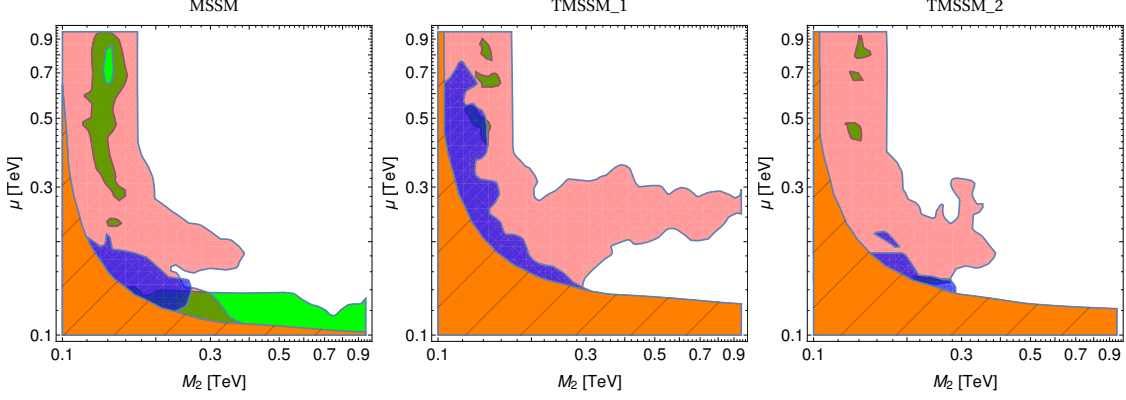
**Figure 1**. Left: Excluded regions at 95% CL after the LHC Run 1 for the MSSM scenario with $\tan\beta = 10$. The green, pink and blue shaded regions are the excluded regions from the two-lepton, three-lepton and four-lepton + MET search respectively, while the shaded orange region denotes the LEP bound on the chargino mass at 95% CL. Other panels: Same as left for the TMSSM_1 ($\lambda = 0.65$, $\mu_\Sigma = 300$ GeV, $\tan\beta = 3$) and TMSSM_2 ($\lambda = 0.65$, $\mu_\Sigma = 350$ GeV, $\tan\beta = 3$) scenarios in the central and right panel respectively. In all panels the lightest neutralino is fixed at $m_{\widetilde{\chi}_1^0} = 63$ GeV.

contribute to the three-lepton signal and produce a large number of events. A similar argument can be applied to understand the exclusion coming from the two-lepton + MET search (green region) in the same ballpark of values of $\mu$ and $M_2$. Again several processes ($pp \to \widetilde{\chi}_2^0\widetilde{\chi}_1^0$, $pp \to \widetilde{\chi}_3^0\widetilde{\chi}_1^0$, $pp \to \widetilde{\chi}_3^0\widetilde{\chi}_2^0$, $pp \to \widetilde{\chi}_1^+\widetilde{\chi}_1^-$) contribute to the two-lepton + MET signal, producing numerous events. The most sensitive SR of this latter search is SRWWa. The same corner of the $\{\mu, M_2\}$-plane is constrained by the four-lepton search (blue region). The process giving rise to four-lepton + MET in the final state is $pp \to \widetilde{\chi}_3^0\widetilde{\chi}_2^0$, which is very sensitive to the value of $M_2$ and $\mu$. As soon as one of these parameters increases, $\widetilde{\chi}_3^0$ becomes heavy and its production cross section drops down, reducing drastically the signal. The most sensitive SRs of this search are SR0Z and SR0noZb, which have the largest number of signal events.

Moving to the top left part of the plot (left panel of Fig. 1), the excluded region with light $M_2$ is basically insensitive to the value of $\mu$, as soon as $\mu > 300$ GeV: here only $\widetilde{\chi}_1^\pm$ and $\widetilde{\chi}_2^0$ (which are mostly Wino) can be produced with a significant cross section as they are always light no matter the value of $\mu$. Hence there is only one relevant process that contributes to the three-lepton signal ($pp \to \widetilde{\chi}_1^\pm\widetilde{\chi}_2^0$), see e.g. the benchmark point MSSM_p3 in Tab. 2. Similarly, only lightest chargino production is responsible for the region excluded by the two-lepton + MET search in the parameter space with low $M_2$ and large $\mu$.

The two-lepton + MET search is complementary to the three-lepton + MET search as it is sensitive to the region with low $\mu \gtrsim 150$ GeV and large $M_2 \gtrsim 300$ GeV, which is basically independent of the value of the Wino mass. This case is exemplified by the benchmark point MSSM_p1 in Tab. 2. As shown in the table, there are several processes that can produce two-lepton + MET signals while only one able to produce three-lepton + MET final states ($pp \to \widetilde{\chi}_1^\pm\widetilde{\chi}_2^0$). Again the most constraining SR of the two-lepton +

**Table 2**. Details of three MSSM points belonging to the excluded regions at 8 TeV (MSSM_p1: $M_1 = 80$ GeV, $M_2 = 675$ GeV and $\mu = 110$ GeV; MSSM_p2: $M_1 = 78$ GeV, $M_2 = 279$ GeV and $\mu = 122$ GeV; MSSM_p3: $M_1 = 62$ GeV, $M_2 = 141$ GeV and $\mu = 900$ GeV). All benchmarks have $m_{\widetilde{\chi}_1^0} = 63$ GeV ($\sim$ Bino) and $\tan\beta = 10$. We indicate only the channels with a production cross sections $\sigma > 0.1$ pb and only the BRs larger than 0.01.

| Model | Mass [GeV] | Cross section [pb] | Branching ratios [%] |
|---|---|---|---|
| MSSM_p1 | $m_{\widetilde{\chi}_2^0} = 120$ ($\sim$ Higgsino) | $\sigma(pp \to \widetilde{\chi}_2^0\widetilde{\chi}_1^0) = 0.52$ | BR($\widetilde{\chi}_2^0 \to q\bar{q}\widetilde{\chi}_1^0$) = 0.68 <br> BR($\widetilde{\chi}_2^0 \to l^+l^-\widetilde{\chi}_1^0$) = 0.11 <br> BR($\widetilde{\chi}_2^0 \to \nu\bar{\nu}\widetilde{\chi}_1^0$) = 0.21 |
| | $m_{\widetilde{\chi}_3^0} = 132$ ($\sim$ Higgsino) | $\sigma(pp \to \widetilde{\chi}_3^0\widetilde{\chi}_2^0) = 0.31$ | BR($\widetilde{\chi}_3^0 \to q\bar{q}\widetilde{\chi}_1^0$) = 0.57 <br> BR($\widetilde{\chi}_3^0 \to l\bar{l}\widetilde{\chi}_1^0$) = 0.25 <br> BR($\widetilde{\chi}_3^0 \to qq'\widetilde{\chi}_1^\pm$) = 0.12 <br> BR($\widetilde{\chi}_3^0 \to ll'\widetilde{\chi}_1^\pm$) = 0.058 |
| | $m_{\widetilde{\chi}_1^+} = 111$ ($\sim$ Higgsino) | $\sigma(pp \to \widetilde{\chi}_1^+\widetilde{\chi}_1^-) = 0.78$ <br> $\sigma(pp \to \widetilde{\chi}_1^\pm\widetilde{\chi}_1^0) = 0.59$ <br> $\sigma(pp \to \widetilde{\chi}_1^\pm\widetilde{\chi}_2^0) = 0.59$ | BR($\widetilde{\chi}_1^\pm \to q\bar{q}'\widetilde{\chi}_1^0$) = 0.67 <br> BR($\widetilde{\chi}_1^\pm \to \nu l'\widetilde{\chi}_1^0$) = 0.33 |
| MSSM_p2 | $m_{\widetilde{\chi}_3^0} = 136$ ($\sim$ Higgsino) | $\sigma(pp \to \widetilde{\chi}_3^0\widetilde{\chi}_1^0) = 0.30$ <br> $\sigma(pp \to \widetilde{\chi}_3^0\widetilde{\chi}_2^0) = 0.24$ | BR($\widetilde{\chi}_3^0 \to q\bar{q}\widetilde{\chi}_1^0$) = 0.68 <br> BR($\widetilde{\chi}_3^0 \to l^+l^-\widetilde{\chi}_1^0$) = 0.11 <br> BR($\widetilde{\chi}_3^0 \to \nu\bar{\nu}\widetilde{\chi}_1^0$) = 0.21 |
| | $m_{\widetilde{\chi}_1^+} = 114$ ($\sim$ Higgsino) | $\sigma(pp \to \widetilde{\chi}_1^+\widetilde{\chi}_1^-) = 0.84$ <br> $\sigma(pp \to \widetilde{\chi}_1^\pm\widetilde{\chi}_1^0) = 0.55$ <br> $\sigma(pp \to \widetilde{\chi}_1^\pm\widetilde{\chi}_2^0) = 0.42$ <br> $\sigma(pp \to \widetilde{\chi}_1^\pm\widetilde{\chi}_3^0) = 0.42$ | BR($\widetilde{\chi}_1^\pm \to q\bar{q}'\widetilde{\chi}_1^0$) = 0.67 <br> BR($\widetilde{\chi}_1^\pm \to l^\pm\nu_{l'}\widetilde{\chi}_1^0$) = 0.33 |
| MSSM_p3 | $m_{\widetilde{\chi}_1^+} = 150$ ($\sim$ Wino) | $\sigma(pp \to \widetilde{\chi}_1^+\widetilde{\chi}_1^-) = 0.86$ <br> $\sigma(pp \to \widetilde{\chi}_1^\pm\widetilde{\chi}_2^0) = 0.88$ | BR($\widetilde{\chi}_1^\pm \to W^\pm\widetilde{\chi}_1^0$) = 0.99 |

MET search is SRWWa.

The central and right panels of Fig. 1 show the excluded regions for the TMSSM cases under analysis. In both scenarios the most constraining search is the three-lepton + MET search. For the TMSSM_1 (central panel), the three-lepton + MET search excludes the parameter space $200 \,\text{GeV} \lesssim \mu \lesssim 300$ GeV, quite independently of the value of the Wino mass. The rough argument to understand this exclusion is as follow. In this scenario the Triplino mass term is fixed at $\mu_\Sigma = 300$ GeV and a Triplino behaves similarly to a Wino. It is then reasonable to merely exchange $M_2$ with $\mu_\Sigma$ in the MSSM exclusion plot: it is clear that for $\mu \simeq 200$ GeV a value of $\mu_\Sigma$ of 300 GeV is excluded, while $\mu_\Sigma \simeq 350$ GeV is still allowed by current searches. Hence we can also argue that the exclusion contours for the TMSSM_2 (right panel), which has $\mu_\Sigma = 350$ GeV, should be closer to the case of the MSSM. This excluded region is indeed only slightly wider than the MSSM case as the EWinos mass spectrum of the TMSSM has a richer content, accordingly there are more processes contributing to the three-lepton + MET final state. In general the most sensitive SRs are those with the largest statistics: for instance bin 14 of the SR0$\tau$a of the

**Table 3**. Details for a TMSSM benchmark point ($M_1 = 78$ GeV, $M_2 = 675$ GeV, $\mu = 135$ GeV, $\mu_\Sigma = 300$ GeV and $\lambda = 0.65$) as compared to MSSM_p1. The LSP mass is fixed at 63 GeV and $\tan\beta = 3$. Only BRs above $10^{-2}$ and production cross sections larger than 0.1 pb are reported.

| Mass [GeV] | Composition | Cross section [pb] | Branching ratios [%] |
|---|---|---|---|
| $m_{\widetilde{\chi}_2^0} = 123$ | $\sim$ Higgsino | $\sigma(pp \to \widetilde{\chi}_2^0 \widetilde{\chi}_1^0) = 0.28$ | $\mathrm{BR}(\widetilde{\chi}_2^0 \to q\bar{q}\widetilde{\chi}_1^0) = 0.68$ |
| | | | $\mathrm{BR}(\widetilde{\chi}_2^0 \to l^+l^-\widetilde{\chi}_1^0) = 0.11$ |
| | | | $\mathrm{BR}(\widetilde{\chi}_2^0 \to \nu\bar{\nu}\widetilde{\chi}_1^0) = 0.21$ |
| $m_{\widetilde{\chi}_3^0} = 156$ | $\sim$ Higgsino | $\sigma(pp \to \widetilde{\chi}_3^0 \widetilde{\chi}_2^0) = 0.23$ | $\mathrm{BR}(\widetilde{\chi}_3^0 \to Z\widetilde{\chi}_1^0) = 0.96$ |
| $m_{\widetilde{\chi}_1^\pm} = 117$ | $\sim$ Higgsino | $\sigma(pp \to \widetilde{\chi}_1^+ \widetilde{\chi}_1^-) = 0.92$ | $\mathrm{BR}(\widetilde{\chi}_1^\pm \to q\bar{q}'\widetilde{\chi}_1^0) = 0.67$ |
| | | $\sigma(pp \to \widetilde{\chi}_1^\pm \widetilde{\chi}_1^0) = 0.32$ | $\mathrm{BR}(\widetilde{\chi}_1^\pm \to \nu l'\widetilde{\chi}_1^0) = 0.33$ |
| | | $\sigma(pp \to \widetilde{\chi}_1^\pm \widetilde{\chi}_2^0) = 0.74$ | |
| | | $\sigma(pp \to \widetilde{\chi}_1^\pm \widetilde{\chi}_3^0) = 0.24$ | |

three-lepton + MET search seems to be the most sensitive one to look for a BSM signal, no matter what is the SUSY model under investigation. We will discuss the sensitivity of the bins and SRs of the multi-lepton searches to the LHC run at 13 TeV center-of-mass energy in Sec. 5.2. We provide further details in Appendix A.

We have performed the Monte Carlo simulations also for an additional scenario of the TMSSM, with $\mu_\Sigma = 350$ GeV and increased $\lambda = 0.85$ to assess the impact of changing this parameter. We find that the excluded region is very similar to the TMSSM_2 case, meaning that leptonic final states are rather insensitive to the value of $\lambda$ (namely they most likely arise from $Z$ and $W$ vector boson decays). The relevance of $\lambda$, which is partially responsible of the coupling between EWinos and the Higgs boson, could be however studied by the search for one-lepton and $b$-jets + MET, designed to tag the production of a Higgs boson in the decay of the SUSY particles into the LSP.

For the TMSSM cases, the two-lepton + MET search looses sensitivity with respect to the case of the MSSM in the region with low $\mu$. The TMSSM has an enriched spectrum, with one additional neutralino and one additional chargino. For low $\mu$ there can be a greater number of light EWino states with respect to the MSSM case. This has the effect of adding new processes to the three-lepton + MET signal, while keeping constant the number of processes contributing to the two-lepton + MET final state, as shown in Tab. 3, hence reducing the sensitivity of the latter search. Still the most relevant SR for the two-lepton + MET search is SRWWa.

To summarize, the most stringent constraints on the EWino parameter space are set by the three-lepton + MET search, in both the MSSM and the TMSSM models. In the MSSM the two-lepton + MET search is complementary to the three-lepton final state in the region with low $\mu$ and $M_2 \gtrsim 300$ GeV. This complementarity is lost in the TMSSM models, where only the three-lepton + MET search is able to exclude a significant part of the parameter space. Our findings for the excluded regions of the MSSM are compatible with the analysis done in Ref. [35].
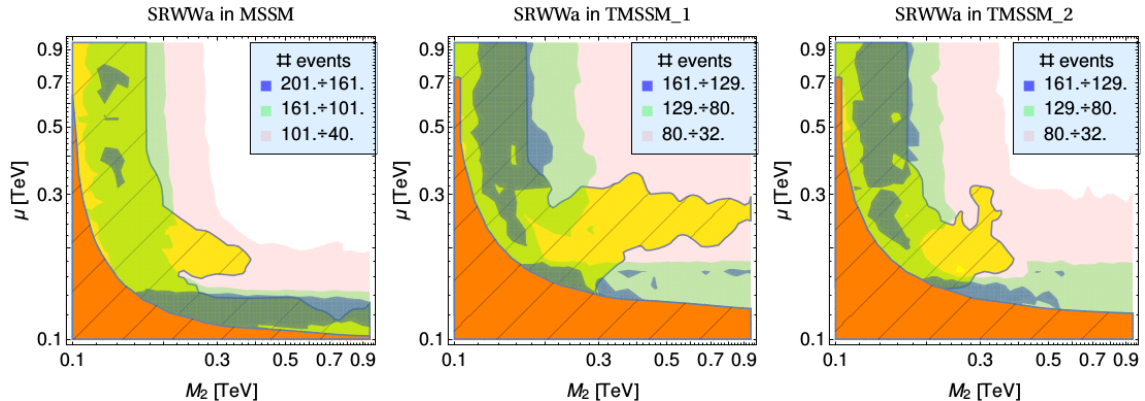
**Figure 2**. Number of expected signal events, as labelled, in the MSSM (left panel), the TMSSM_1 (center panel) and the TMSSM_2 (right panel) in the SRWWa region of the two-lepton analysis. The excluded regions (yellow and orange for the LHC Run 1 bound and chargino mass bound respectively), surrounded by the solid line, are over-imposed.

## 5 Forecasts for multi-lepton signals at the LHC Run 2 and future runs

Searches at the current LHC energy, $\sqrt{s} = 13$ TeV, will probe a much larger region of the parameter space of both the MSSM and the TMSSM, especially for large luminosities. To determine the capabilities of the LHC in the near future, we consider the same searches as in Sec. 3 and estimate the excess of events over the SM expectations in each SR. The complete results are provided in Appendix A. Here we highlight our major findings.

### 5.1 Ascribing a multi-lepton excess to the EWinos

An illustrative example of the 13 TeV forecasts is shown in Fig. 2. From left to right, the expected number of signal events in the SRWWa region of the two-lepton analysis is plotted for a luminosity of 100 fb$^{-1}$ in the MSSM, the TMSSM_1 and the TMSSM_2, respectively. Orange and yellow regions are ruled out by the LEP chargino lower limit and the Run 1 bound obtained before. In all the three cases, in the regions not yet excluded the expected number of signal events goes up to ~150 events. This is about 10 times larger than the expectation in the first LHC run, a factor of five being due to the luminosity, while the remaining factor of two comes from the enhancement in the production cross section as a result of the energy increasing and the PDFs. The SM background, which is quoted in Sec. 3, is expected to scale similarly. This is relevant for the significance of the signal excess, whose estimate is described in the next section. For the time, we disregard such a quantity and base our discussion on order-of-magnitude arguments.

In several cases the forecasts allow to identify whether an anomaly in the multi-lepton data can or cannot be ascribed to the EWinos (with a Bino-like DM LSP). For illustrative purposes, we restrict the present discussion to the SRWWa, SR0τa-20 and SRnoZb SRs and we assume an excess of ~150 events in SRWWa for a 100 fb$^{-1}$ luminosity. As shown in the Appendix A, if this excess is (exclusively) due the EWinos, no excess above 10 events
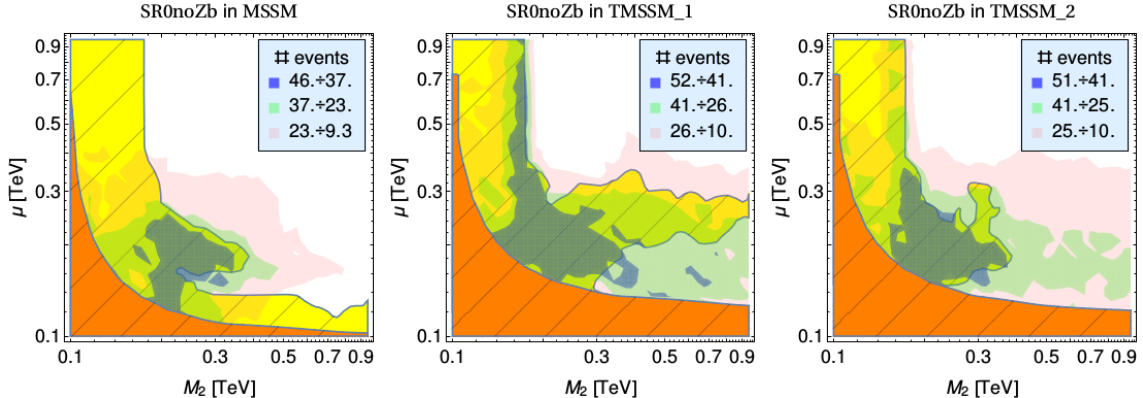
**Figure 3**. Same as Fig. 2 but for the SRnoZb region of the four-lepton analysis.

is possible in SR0τa-20 (here the background is expected to be around 3 events). On the other hand, if this ∼150 excess is accompanied by an anomaly of ∼50 events in SRnoZb (here the background is about 13 events) and a few events in SR0τa-20, the deviation is compatible with the MSSM, TMSSM_1 and TMSSM_2 EWino production, at least for what concerns these three SRs. In particular, the compatibility is possible in the part of $\{\mu, M_2\}$-plane where, for a given model, the blue regions in Figs. 2 and 3 overlap. Of course, to fully test the EWino hypothesis, the compatibility of the excesses in all the SRs must be checked (see Appendix A for more forecast plots). In addition, to quantify the compatibility, the systematic uncertainties involved in the EWino production cannot be disregarded [5]. In this sense, all the numbers of expected signal events in our forecast plots should be used up to a common normalization factor. The statistical uncertainty must also be considered, and this can be done as explained in the next section.

## 5.2 Disentangling the TMSSM from the MSSM

In light of the previous results, one might wonder whether the TMSSM (in one of its scenarios) can be distinguished from the MSSM if an excess is indeed observed in future data. The difficulties for addressing this question are two-fold. On the one hand, the measurement of such an excess is subject to statistical errors due to the potentially large (depending on the SR) background fluctuations. In order to estimate this uncertainty, let us call $D$ the total number of observed events in a particular SR. Let $B$ stands for the number of expected SM events. The number of measured signal events is then given by $S = D - B$ and hence, under the assumption of gaussian distributed events, the uncertainty in $S$ can be estimated to be

$$\Delta S = \sqrt{D + B} = \sqrt{S + 2B}. \tag{5.1}$$

In this way, we can link the uncertainty on $S$ with $S$ itself, provided the number of background events is well known. A similar approach has been adopted in a different context in

---

[5]We compute the EWino production cross sections at leading order.
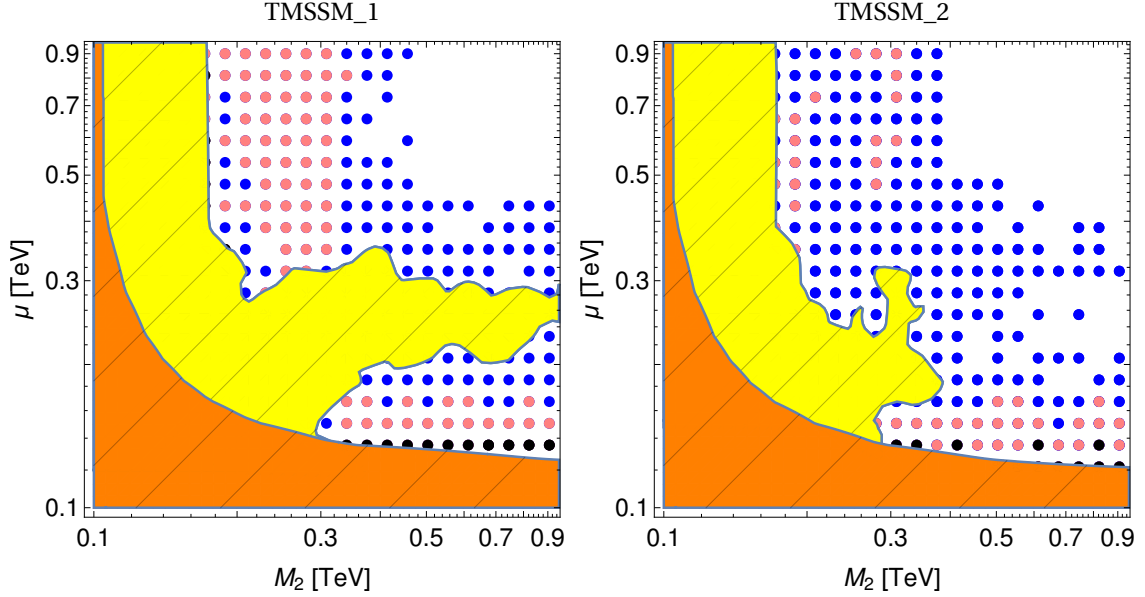
**Figure 4**. Paramater space regions of the TMSSM_1 (left) and the TMSSM_2 (right) that can be disentangled from the MSSM with 100 fb$^{-1}$ (black points), 300 fb$^{-1}$ (red points) and 3000 fb$^{-1}$ (blue points) by comparing bin by bin in all multi-lepton analyses.

Ref. [67]. Given that the multi-lepton production in both the signal and the background is mainly mediated by EW gauge bosons produced in quark-antiquark collisions, we compute the latter simply rescaling the numbers quoted in Sec. 3 by the same amount found for the signal.

On the other hand, it is clear that even the precise measurement of $S$ in a single SR cannot shed light on the nature of the SUSY model, nor on the values of $M_2$ and $\mu$. As a matter of fact, the whole border between the red and the white regions in Fig. 2 in the MSSM correspond to $S \sim 40$ events. A similar number is found in a wide region of the parameter space of both TMSSM scenarios. Therefore, comparing several (potentially all) SRs becomes necessary for disentangling the TMSSM and the MSSM.

Our suggested strategy is as follows. For each parameter space point of the TMSSM, we check whether there exist *at least one* point of the MSSM for which the expected numbers of events in *all* SRs *separately* are compatible, within twice the standard deviation given by Eq. (5.1), with those predicted by the selected value of the TMSSM parameters. If this is *not* the case, the latter can be discriminated from the MSSM. We adopt this approach instead of comparing the whole SR distributions in order the results to be conservative. Indeed, several (uncorrelated) SRs are often involved when a TMSSM parameter point is discriminated from the MSSM.

In the left (right) panel of Fig. 4 we depict the regions of the TMSSM_1 (TMSSM_2) that can be disentangled from the MSSM with 100 fb$^{-1}$ (black points), 300 fb$^{-1}$ (red points) and 3000 fb$^{-1}$ (blue points). It is apparent that most of parameter space region not yet excluded in both versions of the TMSSM would lead to significantly different predictions

from the MSSM ones at the LHC in the long term.

## 6  Conclusions

What are the actual bounds on electroweakinos (EWinos) when the simplified model spectra assumption adopted in the experimental analyses is relaxed? Is there any pattern among the multi-lepton signal regions that events produced by EWinos should follow? In presence of an excess in the multi-lepton channels, is it possible to disentangle among supersymmetric models by means of the details of this pattern? These are the questions we have tackled in the present paper.

To answer to these questions, we have recast the present most contraining analyses on EWinos and applied them to MSSM and Triplet-extension-of-the-MSSM (TMSSM) scenarios with sfermions, gluinos and non-SM Higgses well above the present bounds. Contrarily to the experimental assumptions, no specific EWino mass hierarchy has been assumed. To illustrate our procedure and findings we have chosen a scenario in which the lightest neutralino, Bino-like, is a good dark matter candidate and has a mass in the Higgs funnel region, where LHC is expected to have a better reach and sensitivity with respect to dark matter experiments.

By means of our study we have confirmed that searches for final states with missing transverse energy and two, three or four leptons [31–33] are very efficient to probe light-EWino scenarios [65]. In particular, in the considered MSSM case the present strongest constraints on EWinos, which still come from Run 1 analyses, always result more stringent than the LEP chargino mass bound, $i.e.$ $m_{\widetilde{\chi}^{\pm}} \gtrsim 104\,\mathrm{GeV}$. On the contrary, in the TMSSM, there exists a parameter region (with the Wino and Higgsino mass parameters at $M_2 \gtrsim 300\,\mathrm{GeV}$ and $\mu \simeq 120\,\mathrm{GeV}$, respectively) that evades the LHC multi-lepton constraints and is limited only by the LEP chargino bound.

We have also provided forecasts for the multi-lepton signals produced by the EWino sectors of the MSSM and the TMSSM. For both models we have determined the number of signal events that are expected in each of the signal regions of the multi-lepton analyses above. Irrespectively of the particular MSSM or TMSSM realization, these numbers exhibit some qualitative correlations. These should allow to easily understand whether future anomalies in multi-lepton data are or are not ascribable to EWinos and, in case, what typical values of $\mu$ and $M_2$ can explain the signal.

We have moreover proven that with large enough luminosity the above correlations become precise and sensitive to details of the EWino sector. In some cases, given an EWino signal, it is possible to understand whether the underling theory is the MSSM or some other supersymmetric model with an extended EWino sector. For instance, already at $100\,\mathrm{fb}^{-1}$, there exist a few TMSSM configurations whose EWino signals have correlations that cannot be produced by the MSSM EWinos. This drastically improves at $3000\,\mathrm{fb}^{-1}$: in the considered TMSSM scenario, only the region with $\mu \gtrsim 400\,\mathrm{GeV}$ and $M_2 \gtrsim 400\,\mathrm{GeV}$ leads to signals that can be ascribed also to EWinos of the MSSM.

Interestingly, some searches that we have not investigated in this paper should be sensitive to the large $\mu$ and large $M_2$ parameter region where our procedure fails to disen-

tangle the MSSM from the TMSSM. For instance, the CMS analysis on final states with one lepton and $b$-jets [52] partially covers this parameter space, at least in the MSSM [65]. Also the kinematic observables discussed in Ref. [68] are efficient in probing cases where $\mu$ is large. Therefore, including these extra observables and the one-lepton plus $b$-jet search seems promising and worth investigating in the future.

## Acknowledgments

## A    Relevance of the signal regions in the multi-lepton searches at 13 TeV

In this section we provide a detailed look at the sensitivity of the SRs of each multi-lepton search considered in the analysis for the 13 TeV configuration of the LHC. Before starting to describe the figures, let us define the information contained in each panel. Let us consider at first the top left panel of Fig. 5 as an example. This plot shows the number of signal events produced by the MSSM model in the SR$m_{T2,90}$ of the two-lepton search, in the $\{\mu, M_2\}$-plane. In particular, the blue region shows the number of signal events starting from the 80% of the maximum number of MSSM events up to its maximum, which is in this case 133. The green and pink regions display the number of signal events in between the 50% and 80% of the maximum and in between the 20% and the 50% of the maximum respectively. The panel also shows the exclusion contour (yellow) coming from Run 1, computed as described in Sec. 3.2 as well as the exclusion limit (orange) from LEP on the chargino mass [22] ($m_{\widetilde{\chi}_1^+} \gtrsim 104$ GeV). All panels for the two-lepton, three-lepton and four-lepton search are produced with these details.

### MSSM

Figure 5 shows the sensitivity of the two-lepton and four-lepton searches of the MSSM scenario. For the two-lepton search we have seven SRs (SR$m_{T2,90}$, SR$m_{T2,110}$, SR$m_{T2,150}$,

SRWWa, SRWWb, SRWWc, SRZjets) that corresponds to the first seven panels of Fig. 5. The most relevant SRs are SRWWa, $SRm_{T2,90}$ and SRWWb, in terms of expecting the largest number of signal events. In this scenario, SRWWa is by far the SR with the largest number of expected events, however its sensitivity covers a parameter space in the $\{\mu, M_2\}$-plane which is basically almost completely excluded by LHC Run 1 (if considering as guideline the blue and green shaded regions). Concerning the four-lepton searches the SRs are represented in the last five panels of Fig. 5 (SR0Z, SR1Z, SR0noZa, SR0noZb, SR1noZ). The two SRs with the largest number of predicted events are SR0noZb and SR0Z, however these are less sensitive with respect to the other multi-lepton searches described in our analysis.

The bins of SR0τa of the three-lepton search for the MSSM scenario are represented in Fig. 6. The bins 13 and 14 have the largest predicted number of events and show as well a great capability in exploring the parameter space. It is not granted that the bins with the largest number of predicted events are also the most sensitive. For example, bin 11 has a very large number of signal events, $\mathcal{O}(10^2)$, however the exclusion/exploration potential is very limited and basically coincide with the region already excluded by Run 1. On the other hand we notice that bin 16 can perform well in exploring the model parameter space.

It should be noted that there are several bins with a negligible number of predicted events, which is an additional relevant information that can be used in EWinos searches.

From Figs. 5 and 6 we can infer that the two-lepton and the three-lepton searches are very important for the MSSM scenario in order to find EWino signals at the LHC, while the four-lepton search has a sensitivity which is reduced with respect to the other two searches.

**TMSSM_1 ($\lambda = 0.65$, $\mu_\Sigma = 300$ GeV)**

Figure 7 shows the sensitivity of the two-lepton and the four-lepton searches of the TMSSM_1 scenario previously defined in Sec. 3. As it was the case in the MSSM scenario, the SRs expecting the largest number of signal events are SRWWa, $SRm_{T2,90}$ and SRWWb. However, in this scenario, SRWWc presents a comparable number of events to SRWWa and SRWWb (differently to what happens in the MSSM case). In SRWWa, even though the blue shaded region mostly overlaps with the already existing exclusion limit of Run 1, the green region shows the potential to explore low values of $\mu$ up to 200 GeV irrespective of $M_2$. A complete new region of the parameter space shows up in $SRm_{T2,90}$ and SRWWc, indicating that these two SRs have the capabilities to explore low values of $M_2$ up to 300 GeV irrespective of the value of $\mu$ (blue region). In addition the number of predicted events is very different with respect to the MSSM. For the four-lepton case the bins with the largest number of predicted events are SR0noZb and SR0Z. Despite the fact that this search possesses a reduced sensitivity compared to the other multi-lepton searches, we notice that it seems to have an enhanced potential for discovery for this TMSSM_1 scenario with respect to the MSSM case. This is certainly due to the enriched EWinos mass spectrum augmenting the number of combinations leading to four-lepton + MET signatures.

Figure 8 shows the sensitivity of the bins of SR0τa to the three-lepton signatures of the TMSSM_1 scenario. In this case the bins 13 and 14 have the largest predicted number

of events, similarly to the MSSM case. For this scenario we notice that the number of predicted events is larger than in the MSSM case, as it was explained in Sec. 4. Complementary to those bins, notice that the bin 16 , even though having a much lower number of expected events, can perform better than bin 13 and bin 14 in the region with $\mu$ up to 500 GeV, irrespective on the value of $M_2$ (considering the green shaded region).

**TMSSM_2 ($\lambda = 0.65$, $\mu_\Sigma = 350$ GeV)**

Figure 9 shows the sensitivity of the two-lepton search but now for scenario TMSSM_2, as in Figs. 5 and 7. This scenario behaves similarly to the case of TMSSM_1, still featuring $SRm_{T2,90}$ as a very sensitive SR, even though the number of events is closer to the one of the MSSM scenario. Regarding the four-lepton search, we find results similar to the TMSSM_1 case. The presence of new EWino states modify the decay chains in such a way that different EWino decays contribute to the four-lepton + MET signatures.

The bins of SR0$\tau$a of the three-lepton search for the scenario TMSSM_2 are shown in Fig. 10. The conclusions that can be extracted from this scenario are similar to the ones of the scenario TMSSM_1. The bin 11 is the one with the largest number of signal events, while the bin 16 seems to cover better the parameter region that is not excluded by the LHC Run 1 and it is not reachable in the MSSM scenario. Hence in the three-lepton analysis there are several bins that can be used to look for new physics in general coming from SUSY, irrespective on the details of the model, while there are others, such as bin 16, that are relevant to disentangle among different SUSY models.
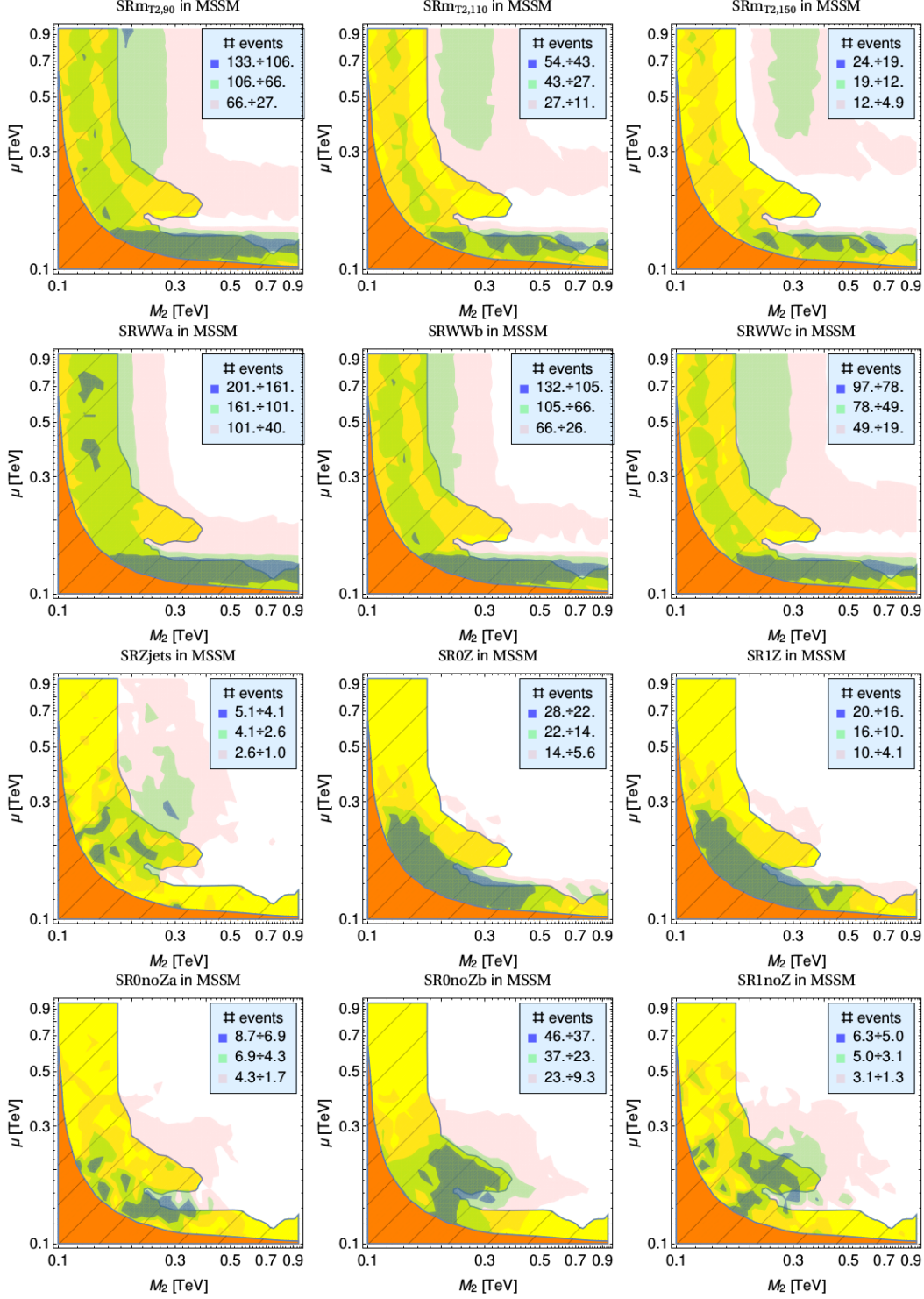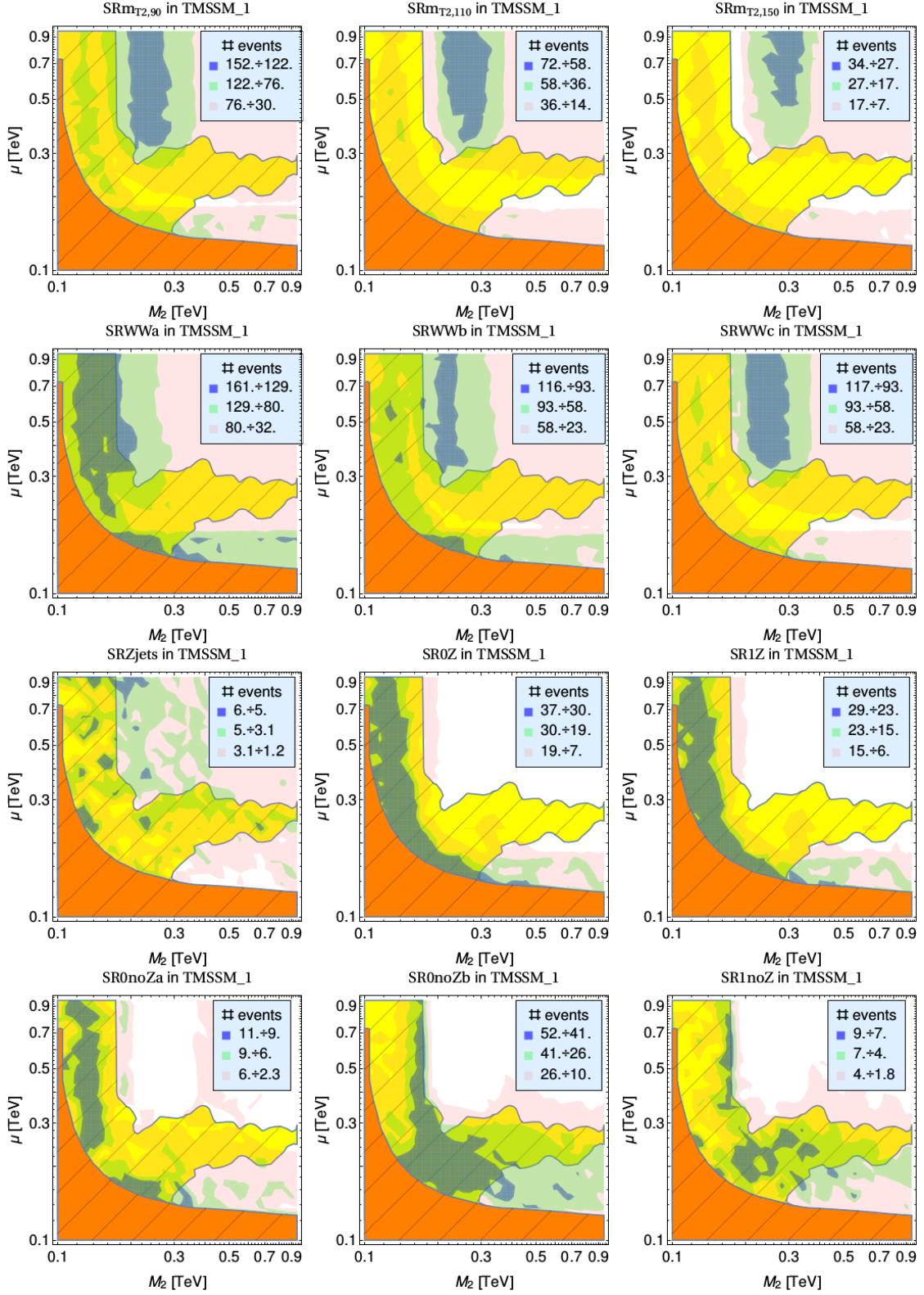
**Figure 5**. **Two-lepton & four-lepton searches - MSSM - 13 TeV:** Number of events in the two-lepton and four-lepton search SRs in the $\{\mu, M_2\}$-plane for the MSSM. From left to right and top to bottom for the two-lepton + MET: $SRm_{T2,90}$, $SRm_{T2,110}$, $SRm_{T2,150}$, SRWWa, SRWWb, SRWWc and SRZjets, as labelled. For the four-lepton case from left to right and top to bottom following the two-lepton SRs: SR0Z, SR1Z, SR0noZa, SR0noZb and SR1noZ. The blue region denotes the number of signal events in the SR in between the maximum and its 80%. The green (pink) regions indicate the number of signal events in between the 50% (20%) and 80% (50%) of its maximum. In yellow we show the region excluded by Run 1, while in orange we denote the excluded region for charginos from LEP.

– 24 –
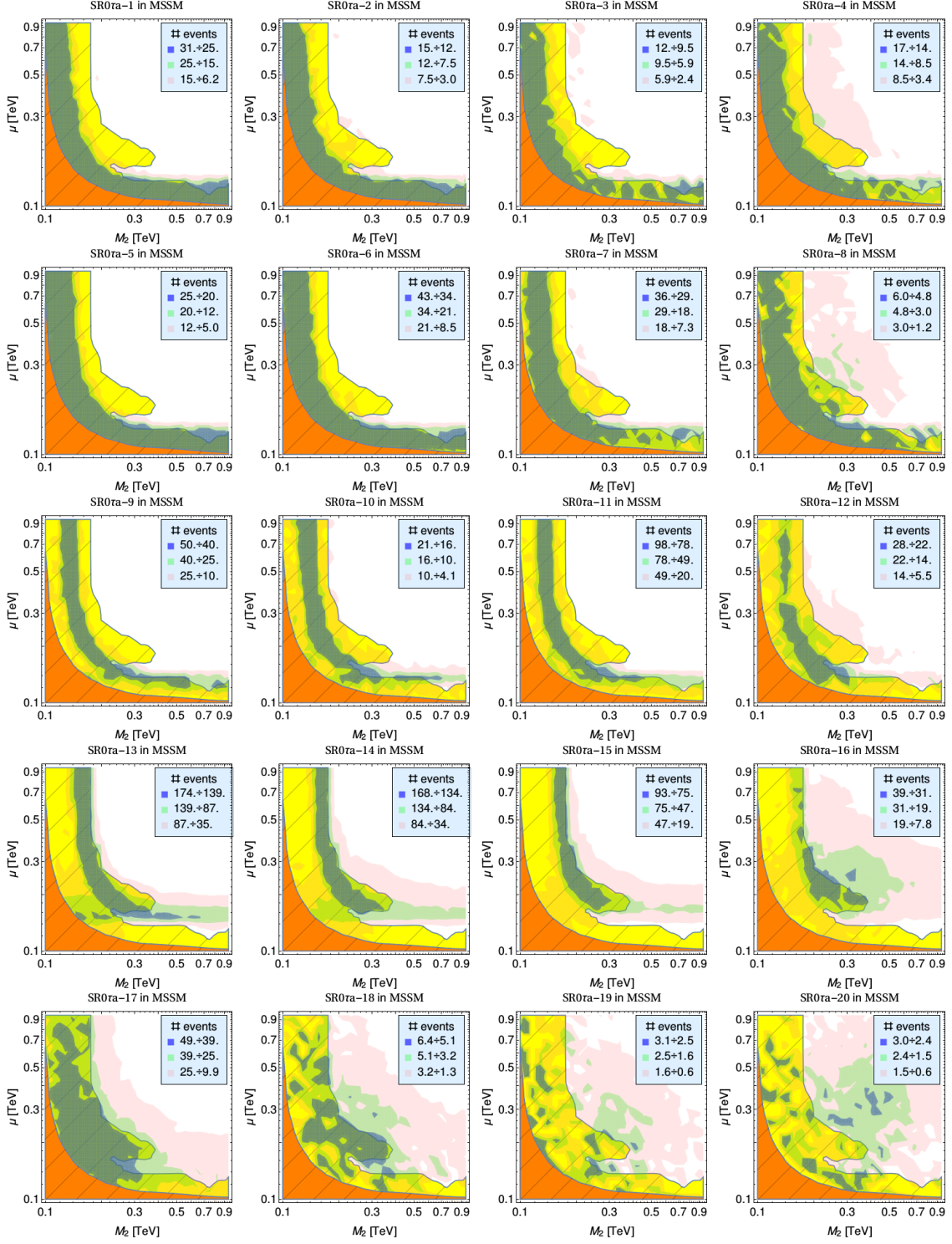
**Figure 6**. **Three-lepton search - MSSM - 13 TeV:** Number of events in the SR0$\tau$ of the three-lepton search in the $\{\mu, M_2\}$-plane for the MSSM. From left to right and top to bottom we show the 20 bins as labelled. The blue region denotes the number of signal events in the SR in between the maximum and its 80%. The green (pink) regions indicate the number of signal events in between the 50% (20%) and 80% (50%) of its maximum. In yellow we show the region excluded by Run 1, while in orange we denote the excluded region for charginos from LEP.

**Figure 7**. **Two-lepton & four-lepton searches - TMSSM_1 - 13 TeV:** Same as Fig. 5 for the TMSSM_1 case ($\lambda = 0.65$ and $\mu_\Sigma = 300$ GeV).
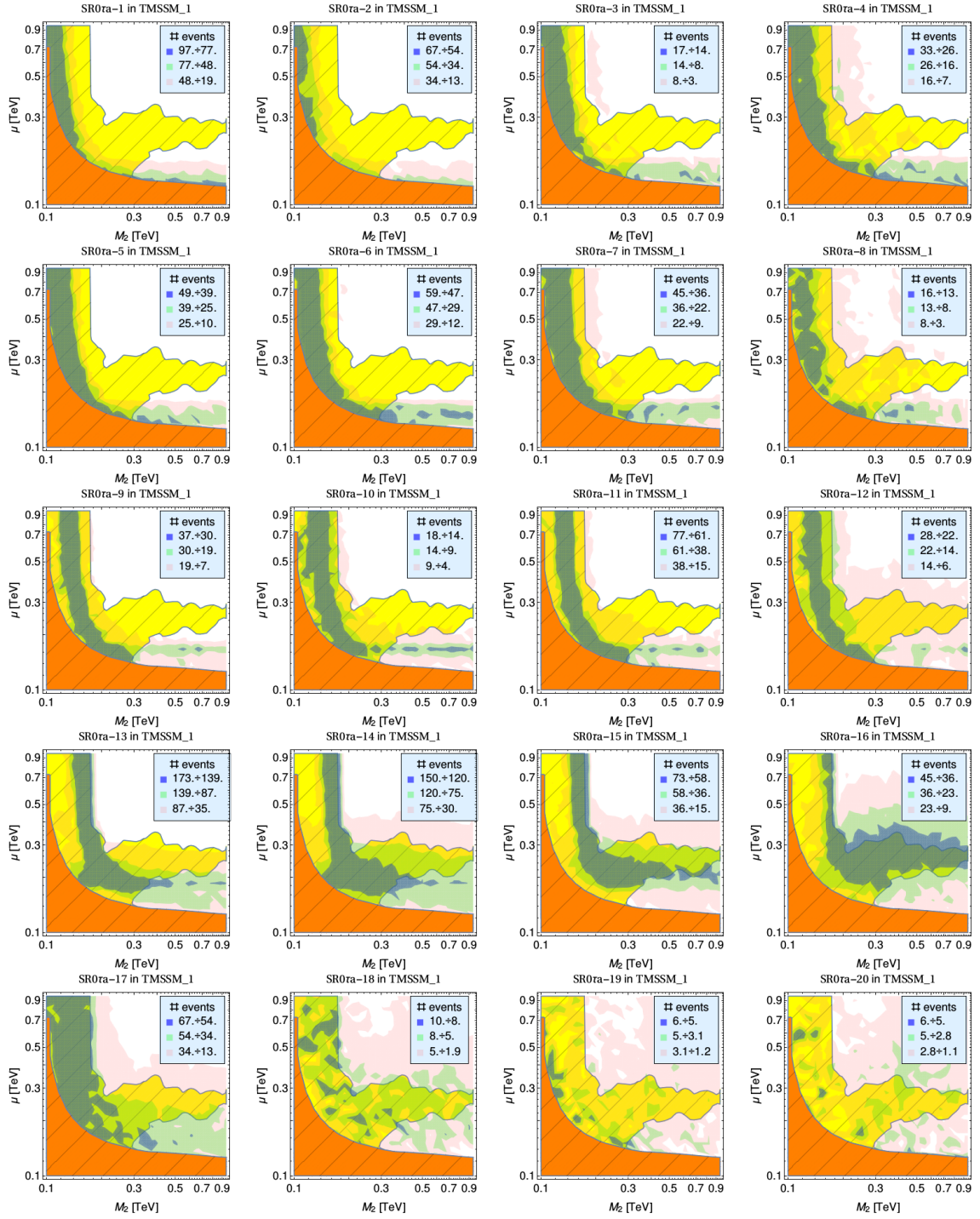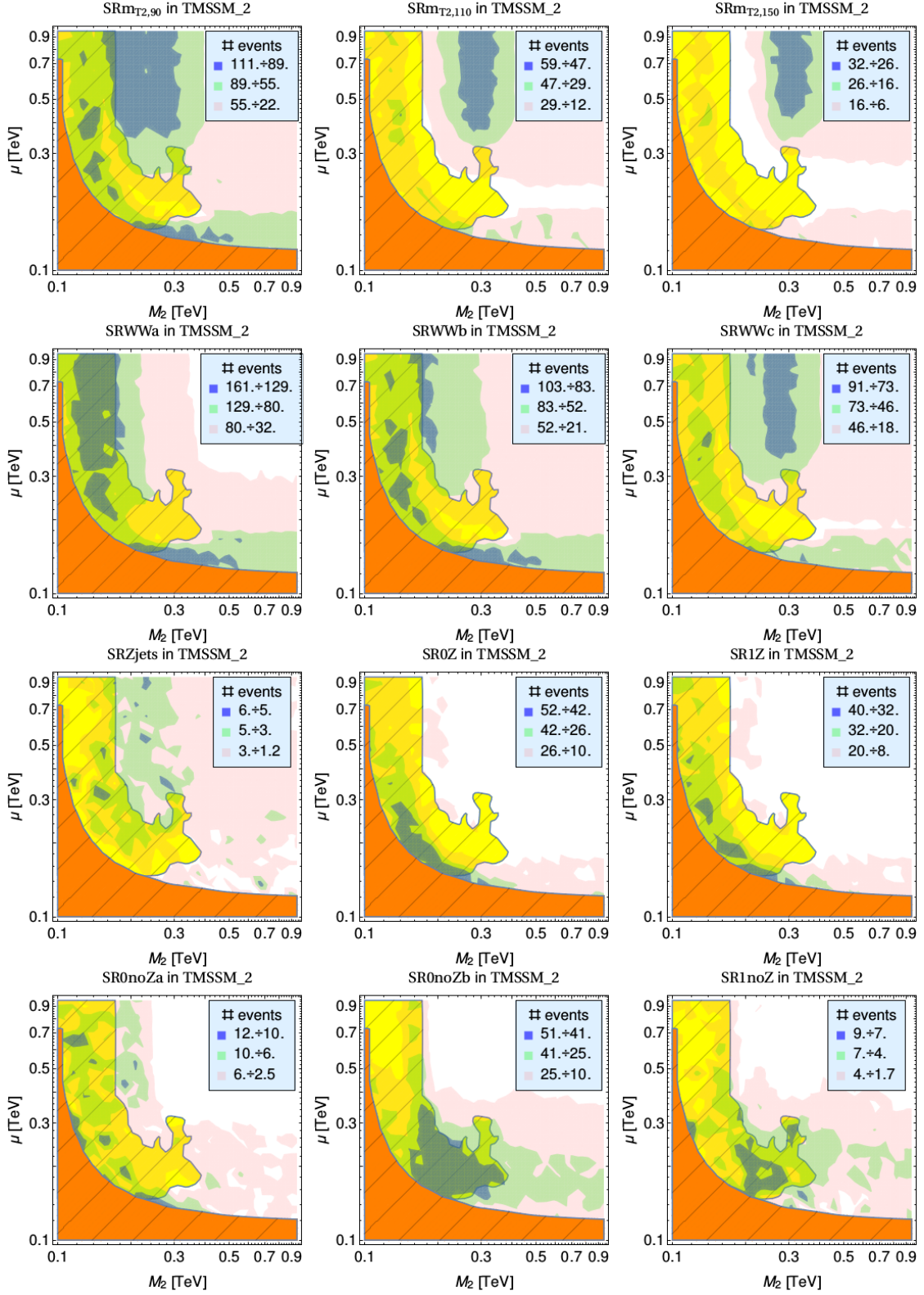
**Figure 8**. **Three-lepton search - TMSSM_1 - 13 TeV:** Same as Fig. 6 for the TMSSM_1 case ($\lambda = 0.65$ and $\mu_\Sigma = 300$ GeV).

**Figure 9**. **Two-lepton & four-lepton searches - TMSSM_2 - 13 TeV:** Same as Fig. 5 for the TMSSM_2 case ($\lambda = 0.65$ and $\mu_\Sigma = 350$ GeV).
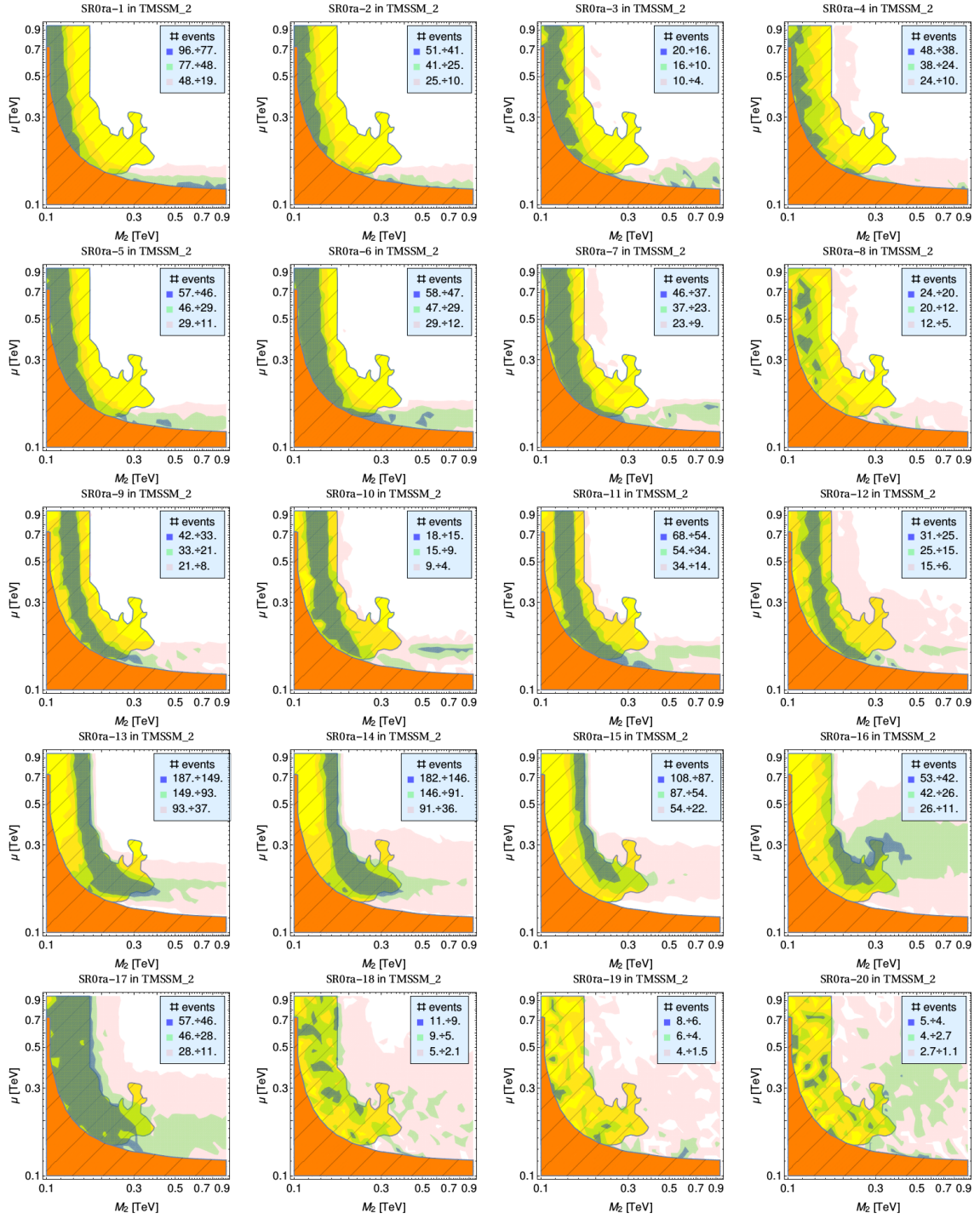
**Figure 10**. **Three-lepton search - TMSSM_2 - 13 TeV:** Same as Fig. 6 for the TMSSM_1 case ($\lambda = 0.65$ and $\mu_\Sigma = 350$ GeV).

# References

[1] **ATLAS** Collaboration, G. Aad et al., *Observation of a new particle in the search for the Standard Model Higgs boson with the ATLAS detector at the LHC*, *Phys.Lett.* **B716** (2012) 1–29, [`arXiv:1207.7214`].

[2] **CMS** Collaboration, S. Chatrchyan et al., *Observation of a new boson at a mass of 125 GeV with the CMS experiment at the LHC*, *Phys.Lett.* **B716** (2012) 30–61, [`arXiv:1207.7235`].

[3] https://twiki.cern.ch/twiki/bin/view/AtlasPublic/SupersymmetryPublicResults.

[4] https://twiki.cern.ch/twiki/bin/view/CMSPublic/PhysicsResultsSUS.

[5] A. Arbey, M. Battaglia, A. Djouadi, F. Mahmoudi, and J. Quevillon, *Implications of a 125 GeV Higgs for supersymmetric models*, *Phys.Lett.* **B708** (2012) 162–169, [`arXiv:1112.3028`].

[6] M. Carena, S. Gori, N. R. Shah, and C. E. Wagner, *A 125 GeV SM-like Higgs in the MSSM and the $\gamma\gamma$ rate*, *JHEP* **1203** (2012) 014, [`arXiv:1112.3336`].

[7] Z. Kang, T. Li, J. Li, and Y. Liu, *A Rediatively Light Stop Saves the Best Global Fit for Higgs Boson Mass and Decays*, `arXiv:1208.2673`.

[8] J. Fan and M. Reece, *A New Look at Higgs Constraints on Stops*, *JHEP* **06** (2014) 031, [`arXiv:1401.7671`].

[9] A. Djouadi and J. Quevillon, *The MSSM Higgs sector at a high $M_{SUSY}$: reopening the low $\tan\beta$ regime and heavy Higgs searches*, *JHEP* **1310** (2013) 028, [`arXiv:1304.1787`].

[10] L. J. Hall and Y. Nomura, *Spread Supersymmetry*, *JHEP* **1201** (2012) 082, [`arXiv:1111.4519`].

[11] G. Giudice and A. Romanino, *Split supersymmetry*, *Nucl.Phys.* **B699** (2004) 65–89, [`hep-ph/0406088`].

[12] G. Bhattacharyya and T. S. Ray, *Naturally split supersymmetry*, *JHEP* **1205** (2012) 022, [`arXiv:1201.1131`].

[13] K. Benakli, L. Darm, M. D. Goodsell, and P. Slavich, *A Fake Split Supersymmetry Model for the 126 GeV Higgs*, *JHEP* **1405** (2014) 113, [`arXiv:1312.5220`].

[14] A. Masiero, S. Profumo, and P. Ullio, *Neutralino dark matter detection in split supersymmetry scenarios*, *Nucl. Phys.* **B712** (2005) 86–114, [`hep-ph/0412058`].

[15] A. Pierce, *Dark matter in the finely tuned minimal supersymmetric standard model*, *Phys. Rev.* **D70** (2004) 075006, [`hep-ph/0406144`].

[16] H. Baer, A. Mustafayev, E.-K. Park, and S. Profumo, *Mixed wino dark matter: Consequences for direct, indirect and collider detection*, *JHEP* **07** (2005) 046, [`hep-ph/0505227`].

[17] N. Arkani-Hamed, A. Delgado, and G. Giudice, *The Well-tempered neutralino*, *Nucl.Phys.* **B741** (2006) 108–130, [`hep-ph/0601041`].

[18] H. Baer, V. Barger, and H. Serce, *SUSY under siege from direct and indirect WIMP detection experiments*, `arXiv:1609.06735`.

[19] M. Cirelli, F. Sala, and M. Taoso, *Wino-like Minimal Dark Matter and future colliders*, *JHEP* **10** (2014) 033, [`arXiv:1407.7058`]. [Erratum: JHEP01,041(2015)].

[20] T. Golling et al., *Physics at a 100 TeV pp collider: beyond the Standard Model phenomena*, `arXiv:1606.00947`.

[21] **CMS** Collaboration, *Search for new physics in the compressed mass spectra scenario using events with two soft opposite-sign leptons and missing momentum energy at 13 TeV*, Tech. Rep. CMS-PAS-SUS-16-025, CERN, 2016.

[22] **Particle Data Group** Collaboration, K. Olive et al., *Review of Particle Physics*, *Chin.Phys.* **C38** (2014) 090001.

[23] J. Espinosa and M. Quiros, *Higgs triplets in the supersymmetric standard model*, *Nucl.Phys.* **B384** (1992) 113–146.

[24] S. Di Chiara and K. Hsieh, *Triplet Extended Supersymmetric Standard Model*, *Phys.Rev.* **D78** (2008) 055016, [arXiv:0805.2623].

[25] A. Delgado, G. Nardini, and M. Quiros, *Large diphoton Higgs rates from supersymmetric triplets*, *Phys.Rev.* **D86** (2012) 115010, [arXiv:1207.6596].

[26] A. Delgado, G. Nardini, and M. Quiros, *A Light Supersymmetric Higgs Sector Hidden by a Standard Model-like Higgs*, *JHEP* **07** (2013) 054, [arXiv:1303.0800].

[27] P. Bandyopadhyay, K. Huitu, and A. Sabanci, *Status of $Y = 0$ Triplet Higgs with supersymmetry in the light of $\sim 125$ GeV Higgs discovery*, *JHEP* **1310** (2013) 091, [arXiv:1306.4530].

[28] C. Arina, V. Martin-Lozano, and G. Nardini, *Dark matter versus $h \to \gamma\gamma$ and $h \to \gamma$ with supersymmetric triplets*, *JHEP* **1408** (2014) 015, [arXiv:1403.6434].

[29] U. Ellwanger and C. Hugonie, *Higgs bosons near 125 GeV in the NMSSM with constraints at the GUT scale*, *Adv.High Energy Phys.* **2012** (2012) 625389, [arXiv:1203.5048].

[30] A. Delgado, M. Garcia-Pepin, G. Nardini, and M. Quiros, *Natural Supersymmetry from Extra Dimensions*, arXiv:1608.06470.

[31] **ATLAS** Collaboration, G. Aad et al., *Search for direct production of charginos, neutralinos and sleptons in final states with two leptons and missing transverse momentum in pp collisions at $\sqrt{s} = 8$ TeV with the ATLAS detector*, *JHEP* **05** (2014) 071, [arXiv:1403.5294].

[32] **ATLAS** Collaboration, G. Aad et al., *Search for direct production of charginos and neutralinos in events with three leptons and missing transverse momentum in $\sqrt{s} = 8TeV$ pp collisions with the ATLAS detector*, *JHEP* **04** (2014) 169, [arXiv:1402.7029].

[33] **ATLAS** Collaboration, *Search for supersymmetry in events with four or more leptons in $21fb^{-1}$ of pp collisions at $\sqrt{s} = 8$ TeV with the ATLAS detector*, Tech. Rep. ATLAS-CONF-2013-036, CERN, Geneva, Mar, 2013.

[34] **ATLAS** Collaboration, G. Aad et al., *Search for supersymmetry in events with four or more leptons in $\sqrt{s} = 8$ TeV pp collisions with the ATLAS detector*, *Phys. Rev.* **D90** (2014), no. 5 052001, [arXiv:1405.5086].

[35] T. A. W. Martin and D. Morrissey, *Electroweakino constraints from LHC data*, *JHEP* **1412** (2014) 168, [arXiv:1409.6322].

[36] H. K. Dreiner, M. Kramer, and J. Tattersall, *How low can SUSY go? Matching, monojets and compressed spectra*, *Europhys.Lett.* **99** (2012) 61001, [arXiv:1207.1613].

[37] J. Fan, M. Reece, and J. T. Ruderman, *Stealth Supersymmetry*, *JHEP* **1111** (2011) 012, [arXiv:1105.5135].

[38] E. A. Bagnaschi et al., *Supersymmetric Dark Matter after LHC Run 1*, *Eur. Phys. J.* **C75** (2015) 500, [arXiv:1508.01173].

[39] **ATLAS, CMS** Collaboration, G. Aad et al., *Combined Measurement of the Higgs Boson Mass in pp Collisions at $\sqrt{s} = 7$ and 8 TeV with the ATLAS and CMS Experiments*, *Phys. Rev. Lett.* **114** (2015) 191803, [arXiv:1503.07589].

[40] F. Staub, *From Superpotential to Model Files for FeynArts and CalcHep/CompHep*, *Comput.Phys.Commun.* **181** (2010) 1077–1086, [arXiv:0909.2863].

[41] F. Staub, *Automatic Calculation of supersymmetric Renormalization Group Equations and Self Energies*, *Comput.Phys.Commun.* **182** (2011) 808–833, [arXiv:1002.0840].

[42] F. Staub, *SARAH 3.2: Dirac Gauginos, UFO output, and more*, *Comput. Phys. Commun.* **184** (2013) pp. 1792–1809, [arXiv:1207.0906]. [Comput. Phys. Commun.184,1792(2013)].

[43] W. Porod, *SPheno, a program for calculating supersymmetric spectra, SUSY particle decays and SUSY particle production at e+ e- colliders*, *Comput.Phys.Commun.* **153** (2003) 275–315, [hep-ph/0301101].

[44] W. Porod and F. Staub, *SPheno 3.1: Extensions including flavour, CP-phases and models beyond the MSSM*, *Comput.Phys.Commun.* **183** (2012) 2458–2469, [arXiv:1104.1573].

[45] J. Alwall, R. Frederix, S. Frixione, V. Hirschi, F. Maltoni, O. Mattelaer, H. S. Shao, T. Stelzer, P. Torrielli, and M. Zaro, *The automated computation of tree-level and next-to-leading order differential cross sections, and their matching to parton shower simulations*, *JHEP* **07** (2014) 079, [arXiv:1405.0301].

[46] **ATLAS** Collaboration, *Search for supersymmetry in events with four or more leptons in $\sqrt{s} = 13$ TeV pp collisions using $13.3\,\text{fb}^1$ of ATLAS data.*, Tech. Rep. ATLAS-CONF-2016-075, CERN, Geneva, Aug, 2016.

[47] **CMS** Collaboration, *Search for electroweak SUSY production in multilepton final states in pp collisions at sqrt(s)=13 TeV with 12.9/fb*, Tech. Rep. CMS-PAS-SUS-16-024, CERN, Geneva, 2016.

[48] **CMS** Collaboration, *Search for SUSY with multileptons in 13 TeV data*, Tech. Rep. CMS-PAS-SUS-16-022, CERN, Geneva, 2016.

[49] **ATLAS** Collaboration, G. Aad et al., *Search for supersymmetry at $\sqrt{s} = 13$ TeV in final states with jets and two same-sign leptons or three leptons with the ATLAS detector*, *Eur. Phys. J.* **C76** (2016), no. 5 259, [arXiv:1602.09058].

[50] **ATLAS** Collaboration, *Search for direct production of charginos and neutralinos in events with three leptons and missing transverse momentum in $21\,\text{fb}^{-1}$ of pp collisions at $\sqrt{s} = 8$ TeV with the ATLAS detector*, Tech. Rep. ATLAS-CONF-2013-035, CERN, Geneva, Mar, 2013.

[51] **CMS** Collaboration, S. Chatrchyan et al., *Search for anomalous production of events with three or more leptons in pp collisions at $\sqrt{(s)} = 8$ TeV*, *Phys. Rev.* **D90** (2014) 032006, [arXiv:1404.5801].

[52] **ATLAS** Collaboration, G. Aad et al., *Search for direct pair production of a chargino and a neutralino decaying to the 125 GeV Higgs boson in $\sqrt{s} = 8$ TeV pp collisions with the ATLAS detector*, *Eur. Phys. J.* **C75** (2015), no. 5 208, [arXiv:1501.07110].

[53] T. Sjostrand, S. Mrenna, and P. Z. Skands, *PYTHIA 6.4 Physics and Manual*, *JHEP* **0605** (2006) 026, [hep-ph/0603175].

[54] **DELPHES 3** Collaboration, J. de Favereau, C. Delaere, P. Demin, A. Giammanco, V. Lemaître, A. Mertens, and M. Selvaggi, *DELPHES 3, A modular framework for fast simulation of a generic collider experiment*, *JHEP* **02** (2014) 057, [arXiv:1307.6346].

[55] E. Conte, B. Fuks, and G. Serret, *MadAnalysis 5, A User-Friendly Framework for Collider Phenomenology*, *Comput. Phys. Commun.* **184** (2013) 222–256, [arXiv:1206.1599].

[56] E. Conte, B. Dumont, B. Fuks, and C. Wymant, *Designing and recasting LHC analyses with MadAnalysis 5*, *Eur. Phys. J.* **C74** (2014), no. 10 3103, [arXiv:1405.3982].

[57] M. Drees, H. Dreiner, D. Schmeier, J. Tattersall, and J. S. Kim, *CheckMATE: Confronting your Favourite New Physics Model with LHC Data*, *Comput. Phys. Commun.* **187** (2014) 227–265, [arXiv:1312.2591].

[58] M. Cacciari and G. P. Salam, *Dispelling the $N^3$ myth for the $k_t$ jet-finder*, *Phys. Lett.* **B641** (2006) 57–61, [hep-ph/0512210].

[59] M. Cacciari, G. P. Salam, and G. Soyez, *FastJet User Manual*, *Eur. Phys. J.* **C72** (2012) 1896, [arXiv:1111.6097].

[60] M. Cacciari, G. P. Salam, and G. Soyez, *The Anti-k(t) jet clustering algorithm*, *JHEP* **04** (2008) 063, [arXiv:0802.1189].

[61] A. L. Read, *Presentation of search results: The CL(s) technique*, *J. Phys.* **G28** (2002) 2693–2704. [,11(2002)].

[62] C. G. Lester and D. J. Summers, *Measuring masses of semiinvisibly decaying particles pair produced at hadron colliders*, *Phys. Lett.* **B463** (1999) 99–103, [hep-ph/9906349].

[63] A. Barr, C. Lester, and P. Stephens, *m(T2): The Truth behind the glamour*, *J. Phys.* **G29** (2003) 2343–2363, [hep-ph/0304226].

[64] H.-C. Cheng and Z. Han, *Minimal Kinematic Constraints and m(T2)*, *JHEP* **12** (2008) 063, [arXiv:0810.5178].

[65] T. A. W. Martin, *Seer: An analysis package for LHCO files*, arXiv:1503.03073.

[66] B. Batell, S. Jung, and C. E. M. Wagner, *Very Light Charginos and Higgs Decays*, *JHEP* **12** (2013) 075, [arXiv:1309.2297].

[67] F. del Aguila, M. Chala, A. Santamaria, and J. Wudka, *Discriminating between lepton number violating scalars using events with four and three charged leptons at the LHC*, *Phys. Lett.* **B725** (2013) 310–315, [arXiv:1305.3904].

[68] M. E. Cabrera, J. A. Casas, and B. Zaldívar, *New techniques for chargino-neutralino detection at LHC*, *JHEP* **08** (2013) 058, [arXiv:1212.5247].